Electronic Supplementary Information (ESI)

Luminescent dinuclear copper(I) complexes bearing 1,4-bis (diphenylphosphino)butane and functionalized 3-(2′-pyridyl)pyrazole mixed ligands

Jing-Lin Chen,[ab]* Zong-Hao Guo,[a] Hua-Guang Yu,[b] Li-Hua He,[a] Sui-Jun Liu,[a] He-Rui Wen,[a] and Jin-Yun Wang [b]*

[a] *School of Metallurgy and Chemical Engineering, Jiangxi University of Science and Technology, Ganzhou 341000, P.R. China*

[b] *State Key Laboratory of Structural Chemistry, Fujian Institute of Research on the Structure of Matter, Chinese Academy of Sciences, Fuzhou 350002, P.R. China*

[c] *College of Physical Science and Technology, Yangzhou University, Yangzhou 225002, P.R. China*

*Authors to whom correspondence should be addressed. E-mail: gzchenjinglin@126.com (J.-L. Chen); jy_wang@fjirsm.ac.cn .

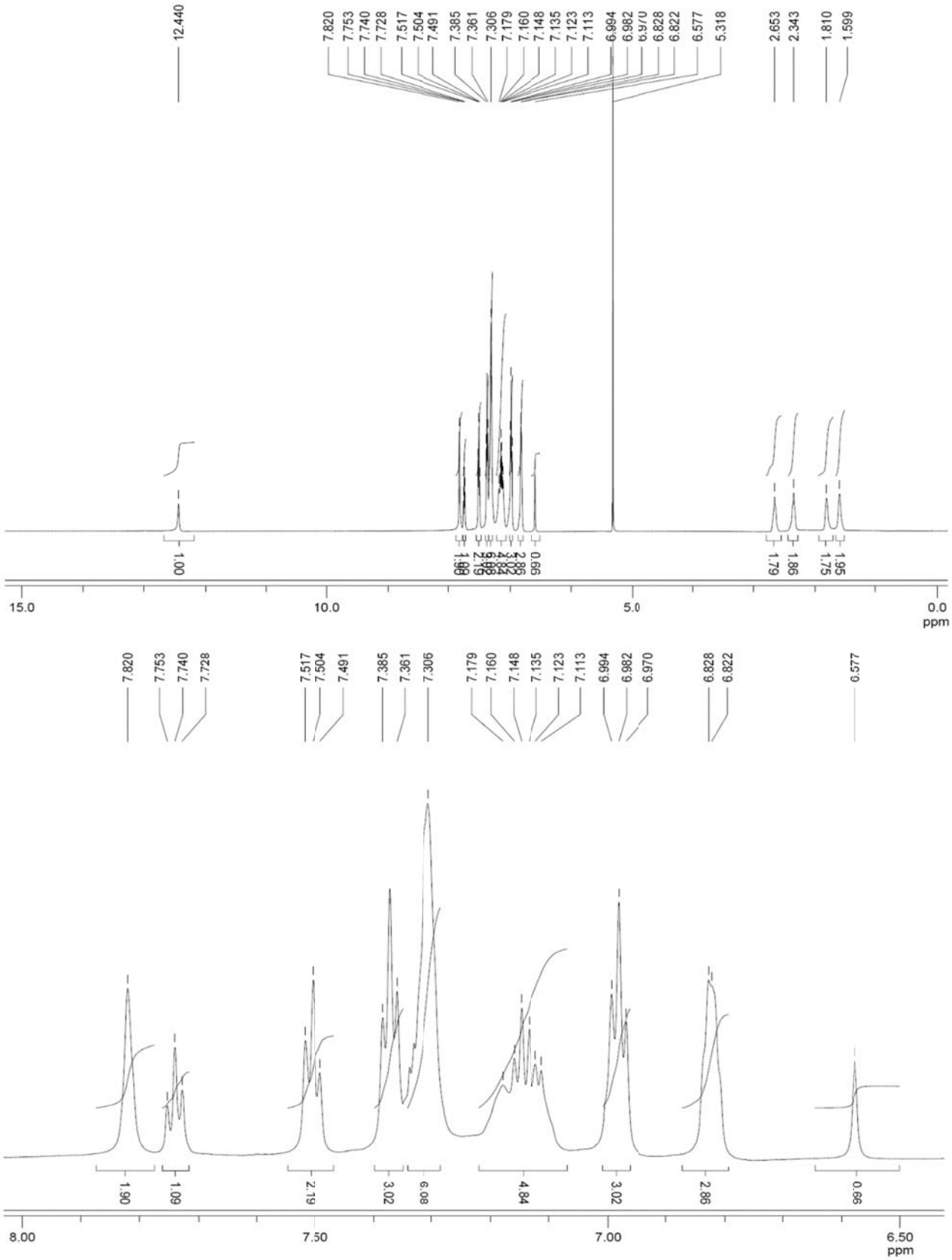

Figure S1 ^{1}H NMR spectra of **1** in CD_2Cl_2.

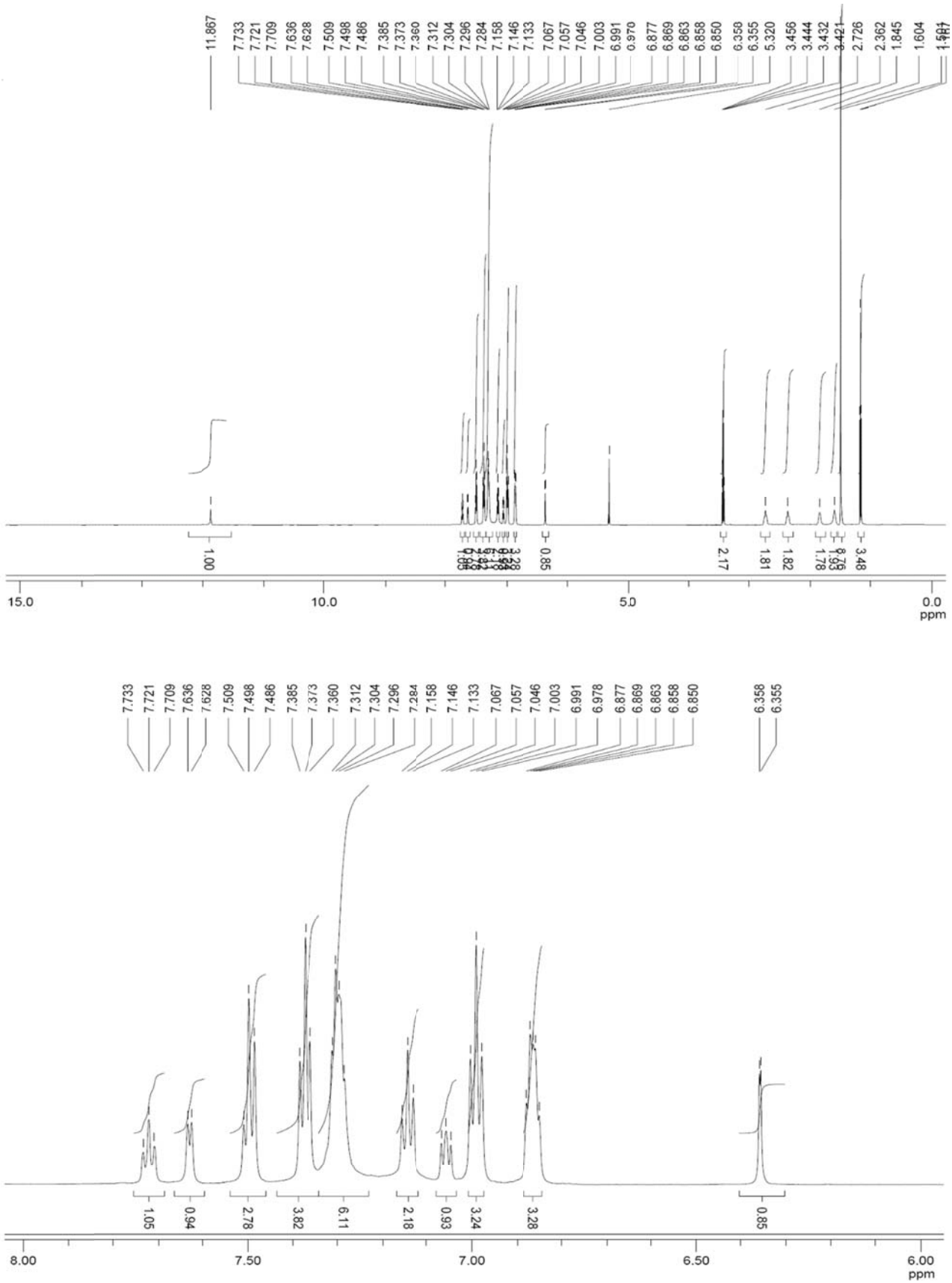

Figure S2 ^{1}H NMR spectra of **2** in CD_2Cl_2.

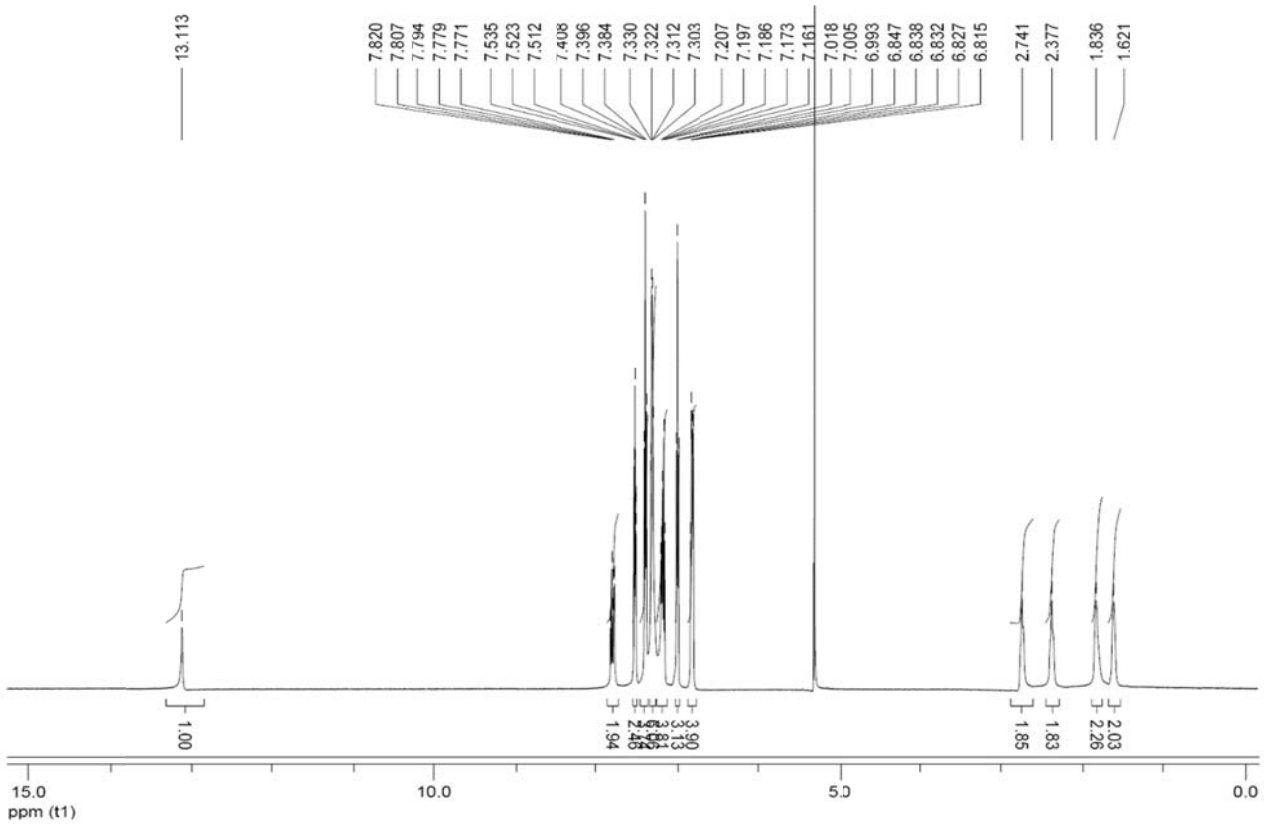

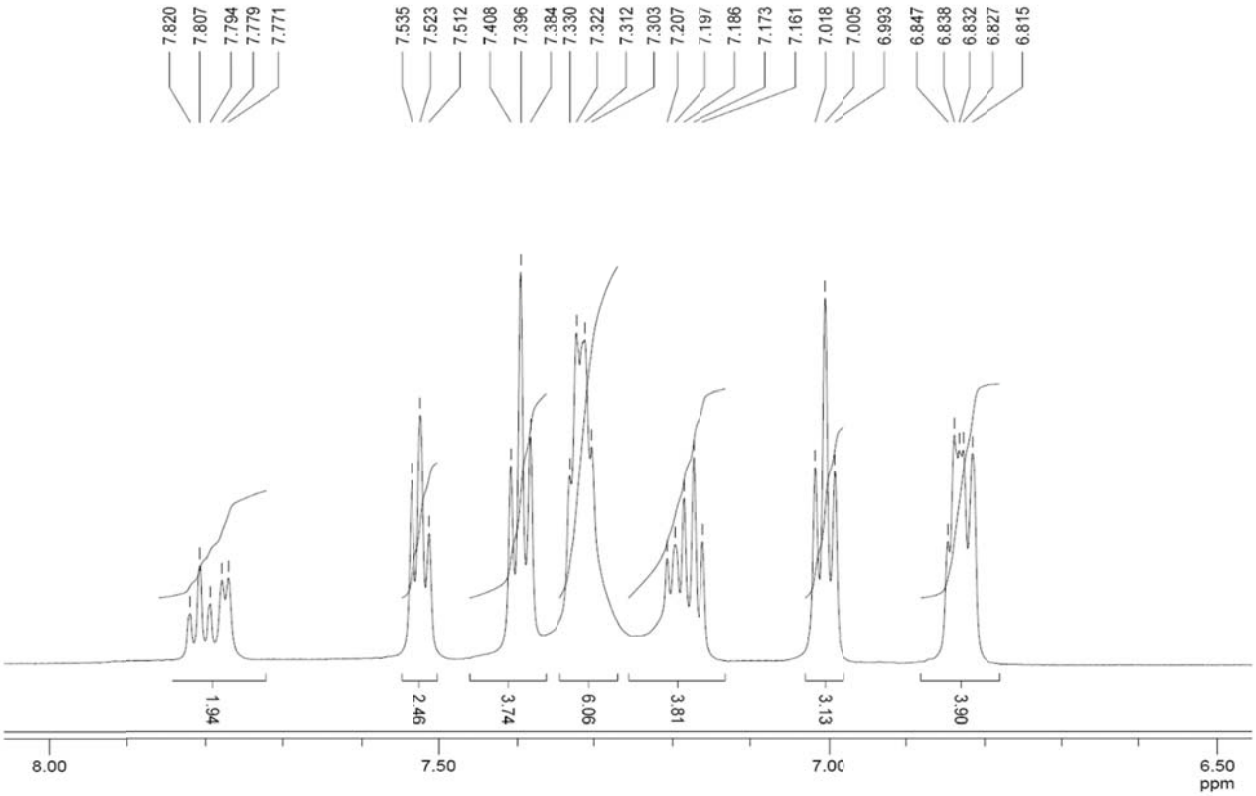

Figure S3 ^{1}H NMR spectra of **3** in CD_2Cl_2.

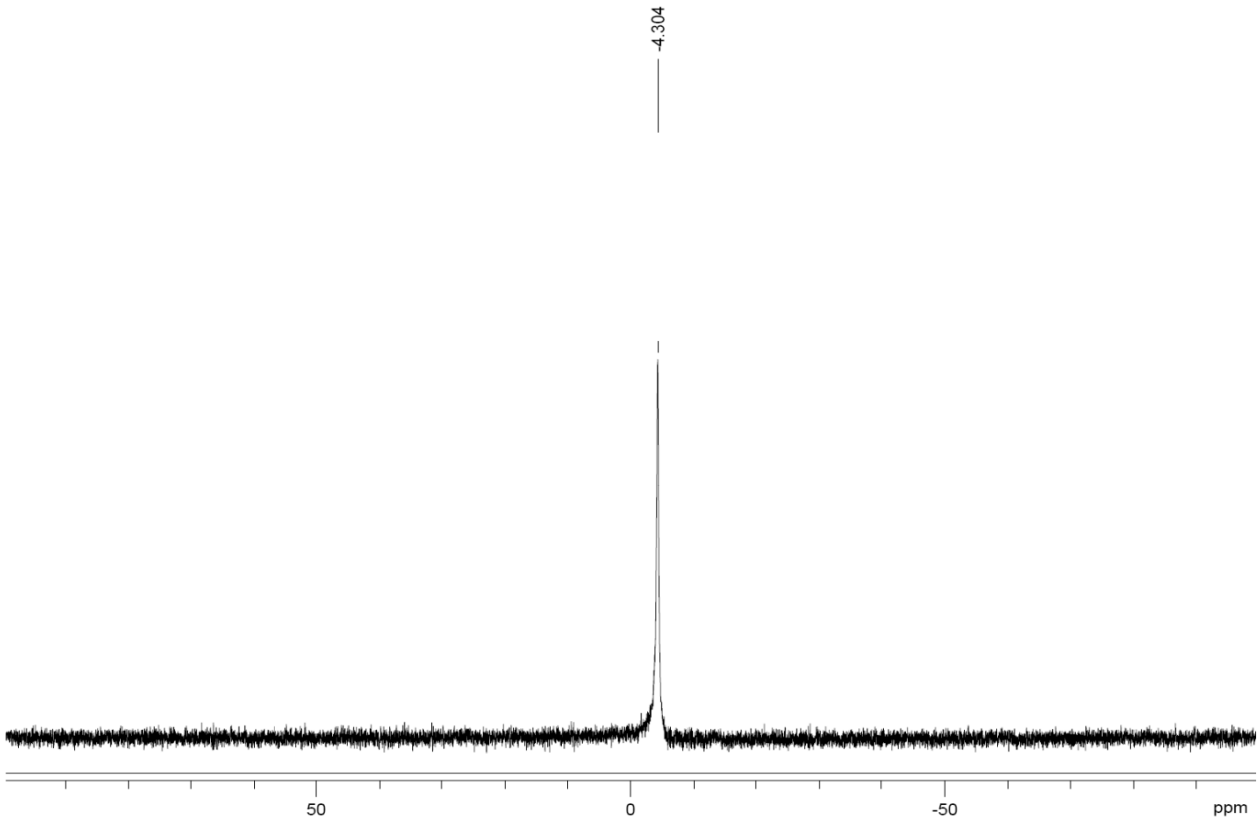

Figure S4 ^{31}P NMR spectrum of **1** in CD_2Cl_2.

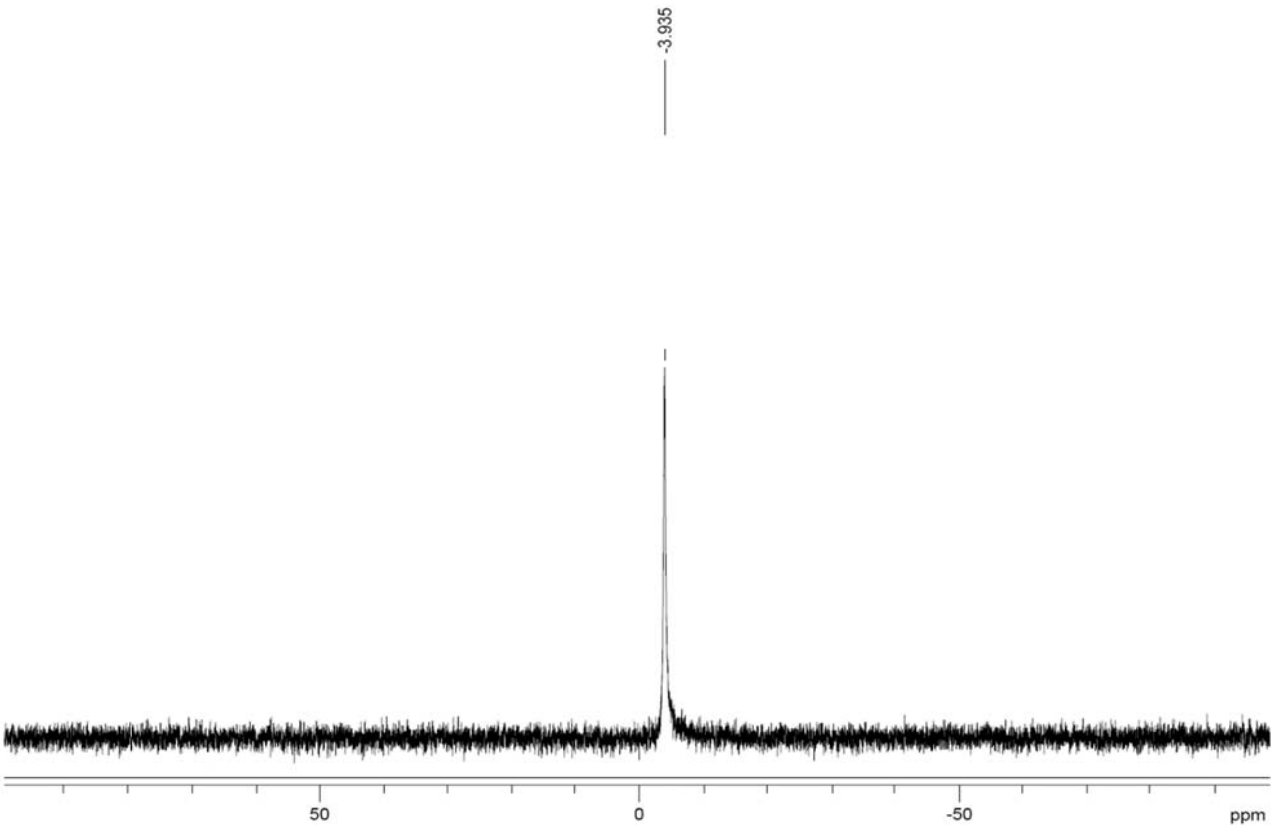

Figure S5 ^{31}P NMR spectrum of **2** in CD_2Cl_2.

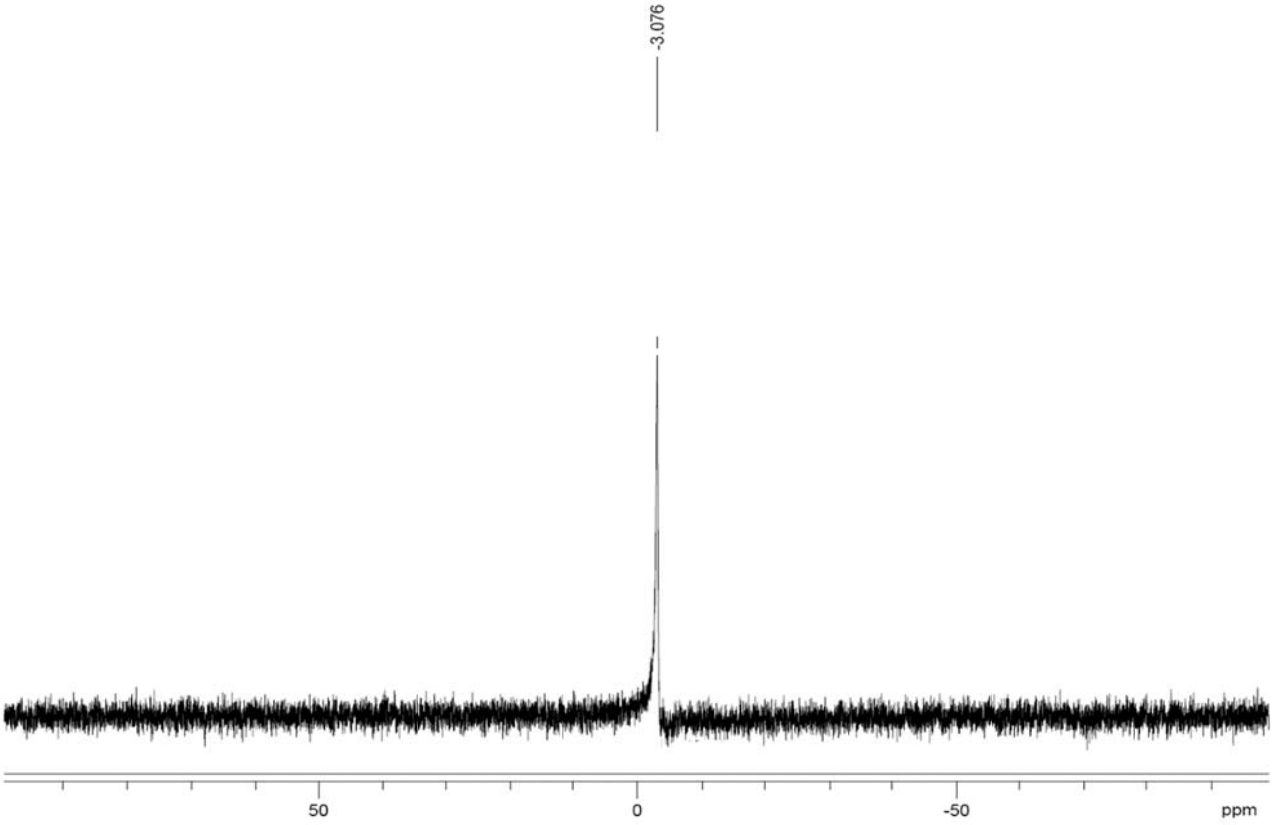

Figure S6 ^{31}P NMR spectrum of **3** in CD_2Cl_2.

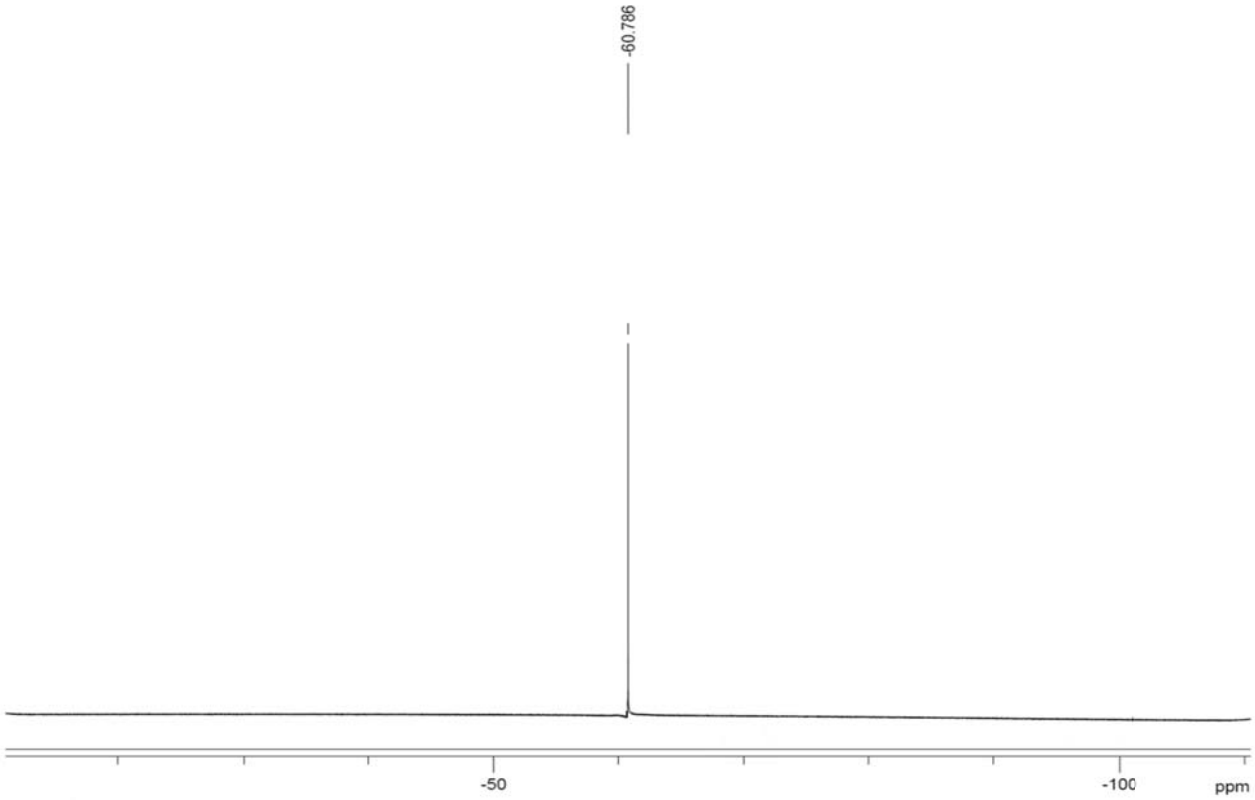

Figure S7 ^{19}F NMR spectrum of **3** in CD_2Cl_2.

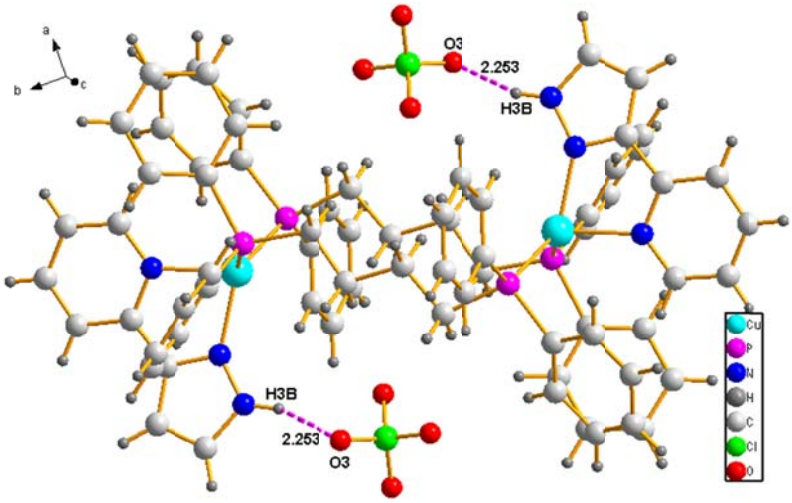

Figure S8 Perspective drawing of **1** with the NH···O hydrogen bond (2.253 Å).

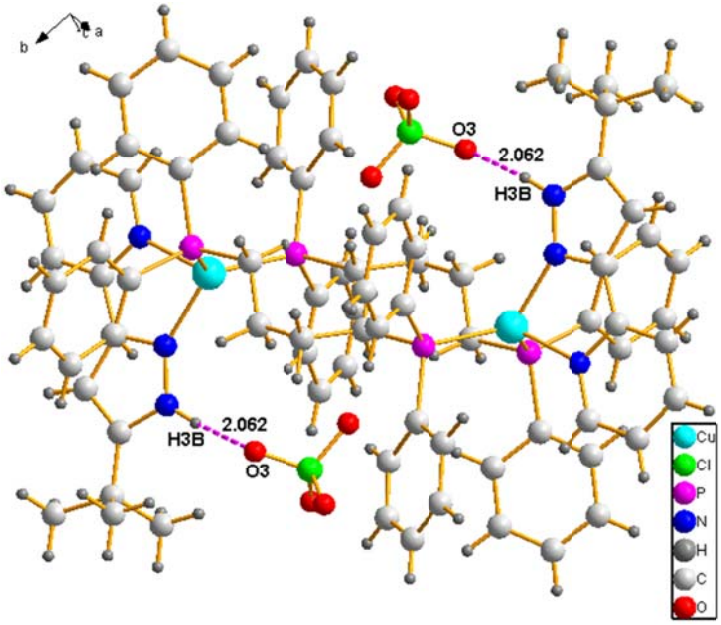

Figure S9 Perspective drawing of **2** with the NH···O hydrogen bond (2.062 Å).

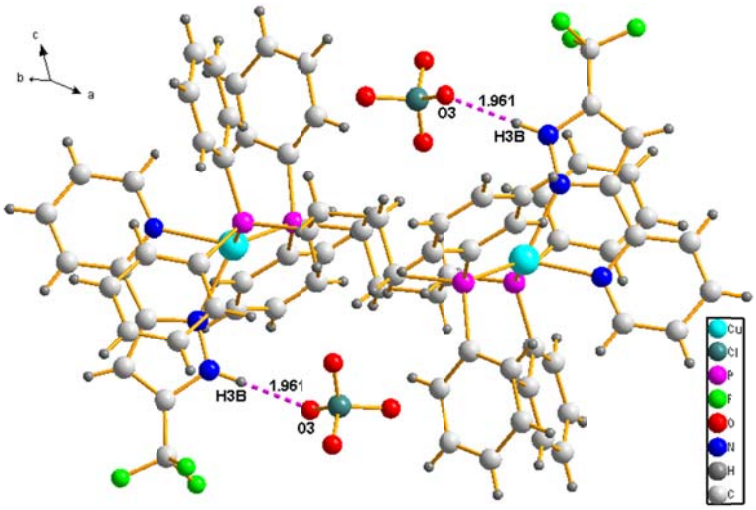

Figure S10 Perspective drawing of **3** with the NH···O hydrogen bond (1.961 Å).

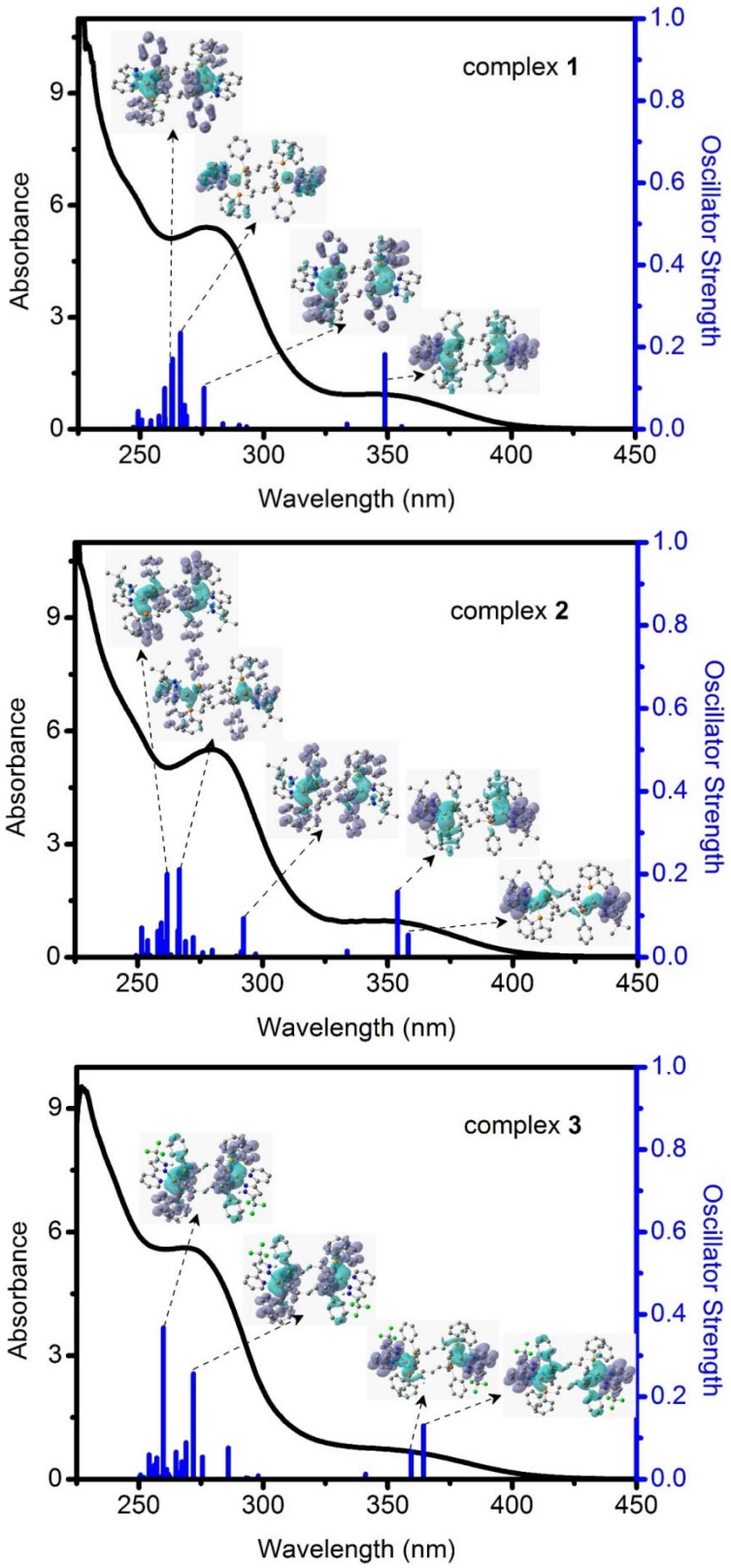

Figure S11 Experimental (solid line) and calculated (vertical lines) absorption spectra in CH_2Cl_2 solution for **1**–**3** by TDDFT method at the B3LYP level. Inset: the charge density difference map (isovalue = 0.0004) between corresponding excited states and the ground states. The purple and blue parts display the electron accumulation and depletion region, respectively.

Table S1 Partial molecular orbital compositions (%) by SCPA approach (C-squared population analysis proposed by Ros and Schuit) and the absorption transitions for **1** in CH_2Cl_2 solution calculated by TDDFT method at the B3LYP level.

orbital	energy (eV)	MO contribution (%)		
		Cu (s/p/d)	dppb	pypzH
LUMO+11	-0.88	5.65 (29/56/15)	91.91	2.44
LUMO+10	-0.89	5.50 (27/62/11)	92.16	2.34
LUMO+7	-1.09	1.23 (41/30/28)	98.20	0.58
LUMO+6	-1.11	3.22 (65/24/11)	95.79	0.99
LUMO+5	-1.17	4.41 (30/47/23)	92.94	2.65
LUMO+4	-1.18	3.14 (19/49/32)	94.71	2.15
LUMO+1	-2.02	2.00 (1/17/83)	4.67	93.32
LUMO	-2.02	1.99 (0/15/84)	4.83	93.18
HOMO	-6.27	45.06 (0/5/95)	49.37	5.56
HOMO-1	-6.27	45.24 (0/5/95)	49.22	5.54
HOMO-2	-6.49	63.77 (2/3/95)	18.83	17.40
HOMO-3	-6.50	66.10 (2/3/95)	15.35	18.55
HOMO-4	-6.63	67.85 (3/2/95)	18.70	13.45
HOMO-5	-6.64	66.72 (3/3/94)	21.15	12.13
HOMO-6	-7.13	35.97 (0/0/99)	9.30	54.73
HOMO-7	-7.13	36.29 (0/0/99)	9.14	54.57
HOMO-12	-7.35	46.03 (0/0/100)	12.66	41.31
HOMO-13	-7.35	47.49 (0/0/100)	11.31	41.20

state	E/nm (eV)	O.S.	transition	assignment	measured value (nm)
S_1	356 (3.49)	0.0000	HOMO-3→LUMO+1 (44%) HOMO-2→LUMO (42%)	^{1}MLCT/^{1}IL/^{1}LLCT	

S_2	356	0.0068	HOMO-3→LUMO (44%)	^{1}MLCT/^{1}IL/^{1}LLCT	
	(3.49)		HOMO-2→LUMO+1 (42%)		
S_3	349	0.1821	HOMO→LUMO (47%)	^{1}LLCT/^{1}MLCT	344
	(3.55)		HOMO-1→LUMO+1 (47%)		
S_{23}	276	0.1004	HOMO→LUMO+6 (46%)	^{1}IL/^{1}MLCT	279
	(4.49)		HOMO-1→LUMO+7 (42%)		
S_{32}	266	0.2342	HOMO-6→LUMO (12%)	^{1}IL/^{1}MLCT	
	(4.65)		HOMO-7→LUMO+1 (11%)		
			HOMO-13→LUMO (10%)		
			HOMO-12→LUMO+1 (9%)		
S_{36}	263	0.1711	HOMO→LUMO+10 (21%)	^{1}IL/^{1}MLCT/^{1}LLCT	
	(4.71)		HOMO-1→LUMO+11 (21%)		
			HOMO-4→LUMO+4 (13%)		
			HOMO-5→LUMO+5 (12%)		

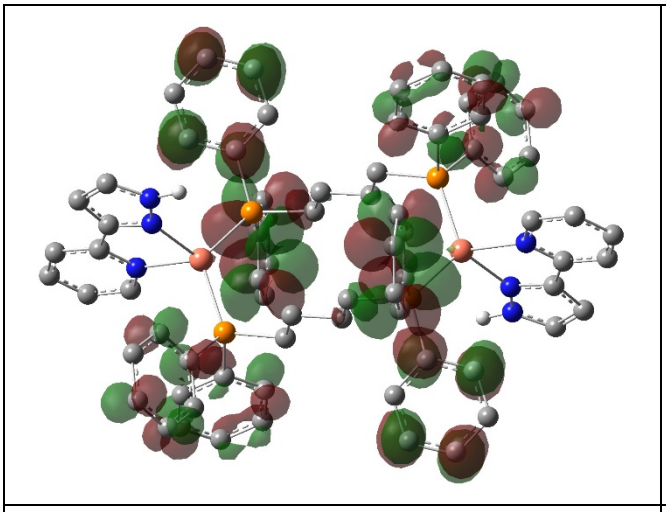	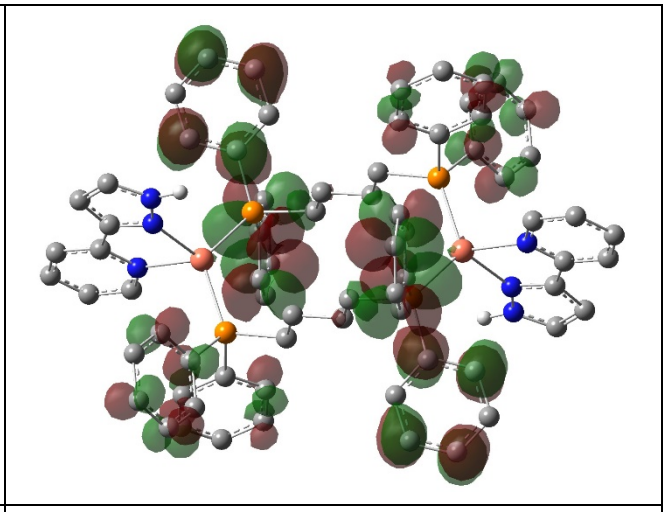
LUMO+11	LUMO+10

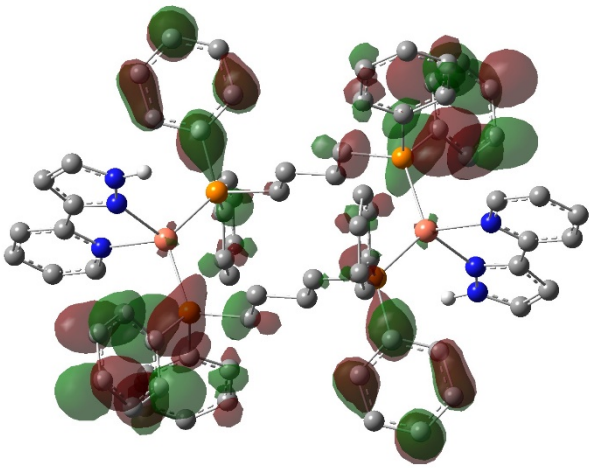	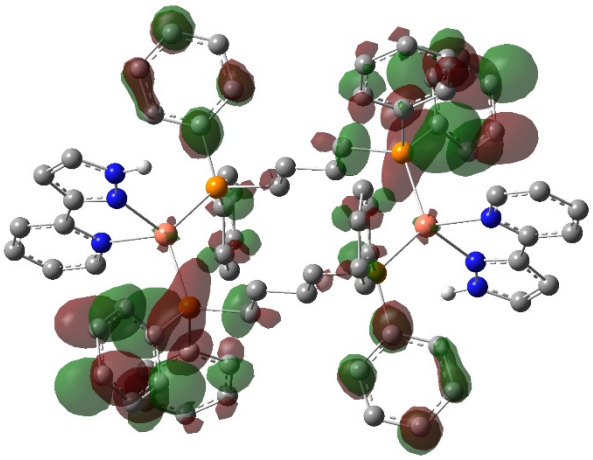
LUMO+7	LUMO+6
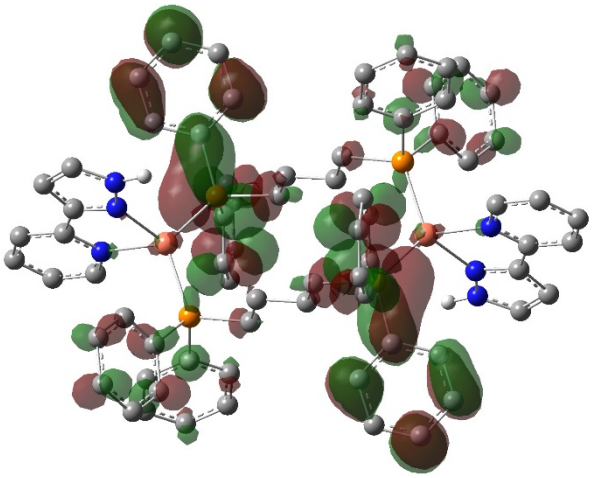	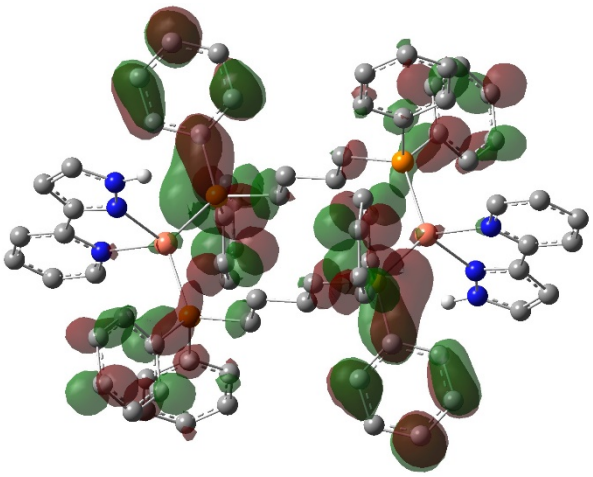
LUMO+5	LUMO+4
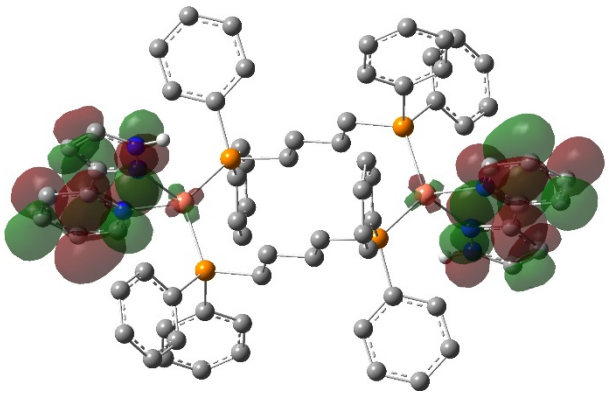	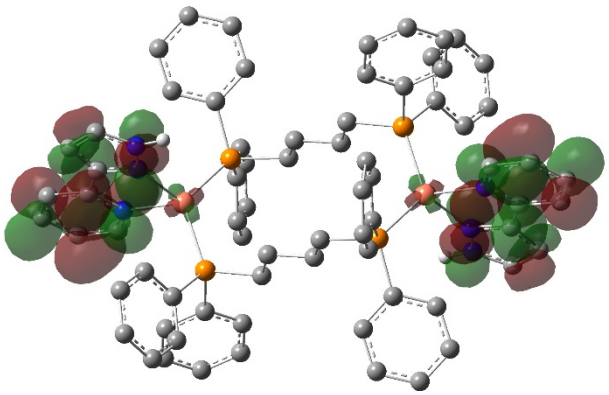
LUMO+1	LUMO

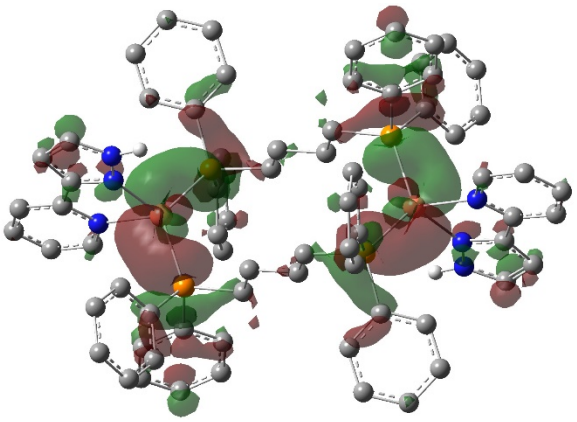	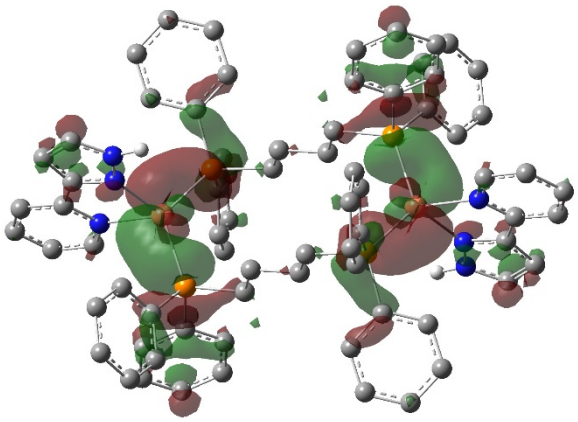
HOMO	HOMO-1
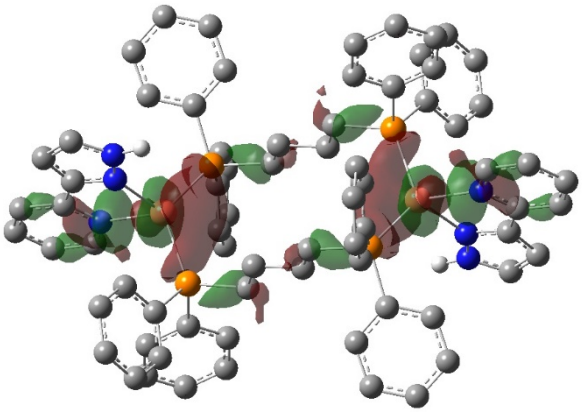	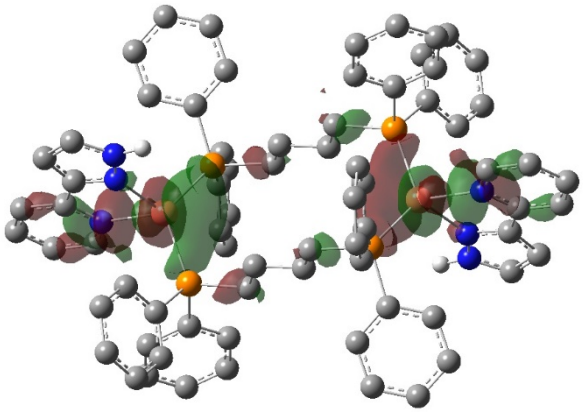
HOMO-2	HOMO-3
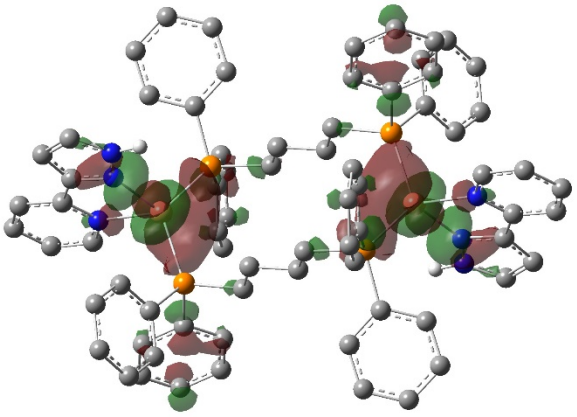	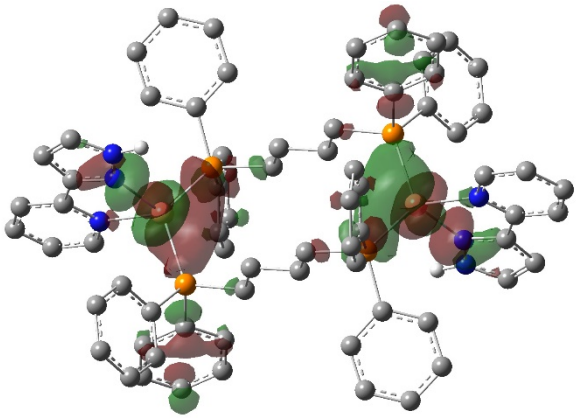
HOMO-4	HOMO-5

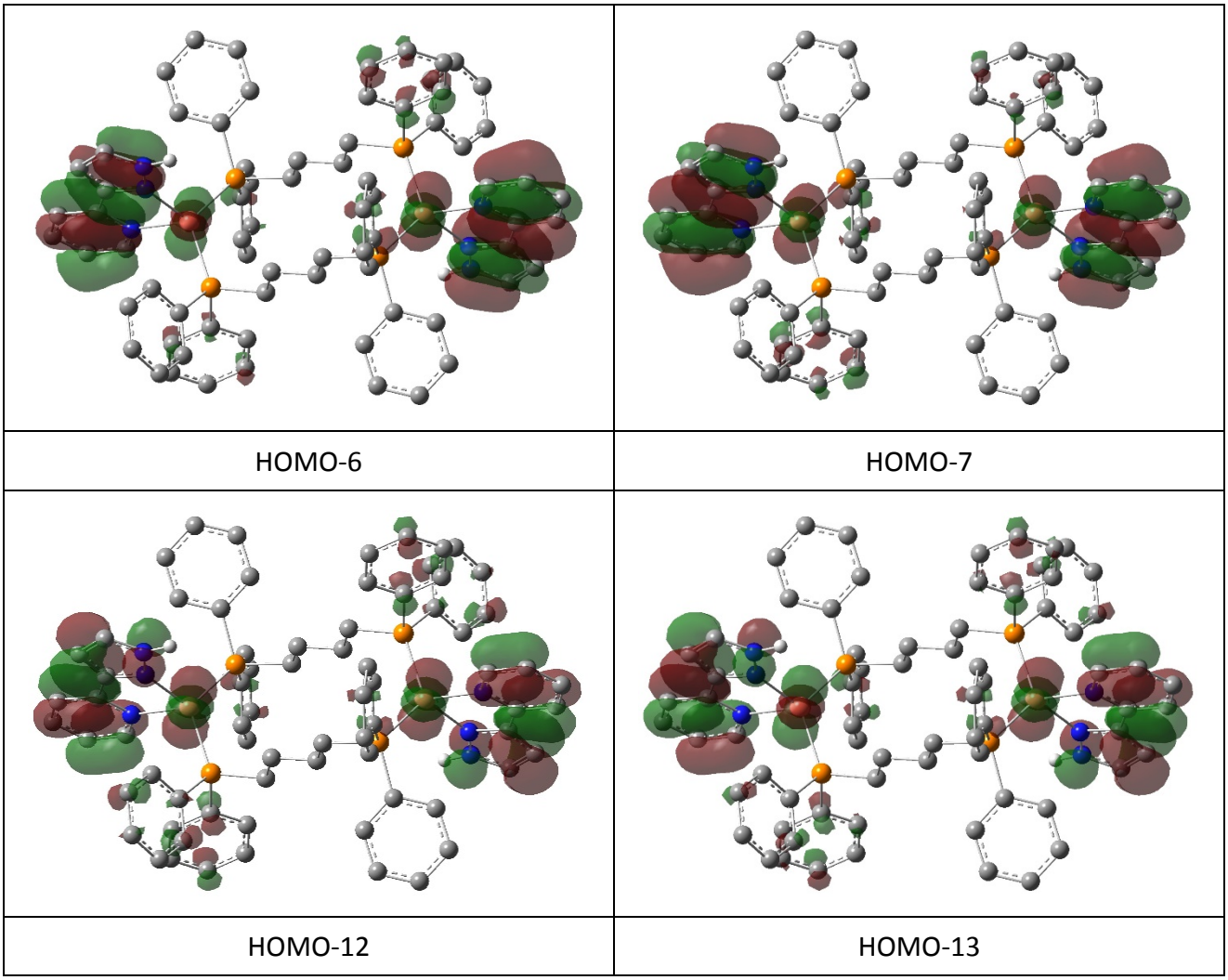

Figure S12 Plots of the frontier molecular orbitals involved in the absorption transitions of **1** in CH_2Cl_2 solution by TDDFT method at the B3LYP level (isovalue = 0.02). For clarity, the hydrogen atoms except for the ones bonded to N atoms are omitted. The red and green parts represent different phases, respectively.

Table S2 Partial molecular orbital compositions (%) by SCPA approach (C-squared population analysis proposed by Ros and Schuit) and the absorption transitions for **2** in CH_2Cl_2 solution calculated by TDDFT method at the B3LYP level.

orbital	energy (eV)	MO contribution (%)		
		Cu (s/p/d)	dppb	pybpzH
LUMO+13	-0.81	2.16 (7/81/12)	95.68	2.16
LUMO+12	-0.82	5.91 (61/33/5)	91.88	2.21
LUMO+5	-1.15	5.52 (33/55/12)	92.06	2.42
LUMO+4	-1.24	7.67 (43/46/10)	89.61	2.72
LUMO+1	-1.99	2.03 (0/15/84)	4.61	93.36
LUMO	-1.99	2.02 (0/15/85)	4.57	93.42
HOMO	-6.16	42.57 (0/6/94)	50.54	6.90
HOMO-1	-6.17	43.01 (0/6/94)	50.09	6.90
HOMO-2	-6.44	63.33 (2/4/94)	19.04	17.63
HOMO-3	-6.46	65.13 (2/3/95)	16.19	18.68
HOMO-4	-6.59	66.55 (3/3/94)	19.97	13.48
HOMO-5	-6.59	65.19 (3/3/94)	22.57	12.25

state	E/nm (eV)	O.S.	transition	assignment	measured value (nm)
S_1	358 (3.46)	0.0539	HOMO-3→LUMO (31%) HOMO-2→LUMO+1 (30%) HOMO-1→LUMO+1 (15%) HOMO→LUMO (15%)	^{1}MLCT/^{1}IL/^{1}LLCT	
S_3	354 (3.50)	0.1572	HOMO→LUMO (35%) HOMO-1→LUMO+1 (33%) HOMO-2→LUMO+1 (14%) HOMO-3→LUMO (13%)	^{1}LLCT/^{1}MLCT/^{1}IL	347
S_{13}	292 (4.24)	0.0936	HOMO→LUMO+4 (60%) HOMO-1→LUMO+5 (35%)	^{1}IL/^{1}MLCT	282

S_{38}	267	0.2111	HOMO-5→LUMO+4 (24%)	^{1}MLCT/^{1}IL/^{1}LLCT
	(4.65)		HOMO-4→LUMO+5 (14%)	
S_{44}	262	0.2002	HOMO→LUMO+12 (40%)	^{1}IL/^{1}MLCT
	(4.74)		HOMO-1→LUMO+13 (39%)	

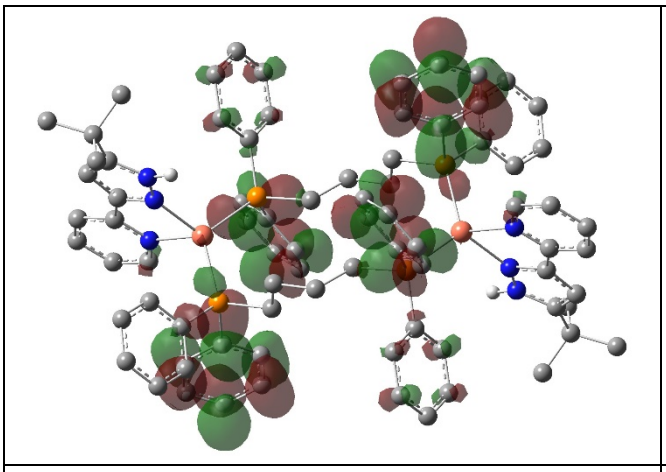	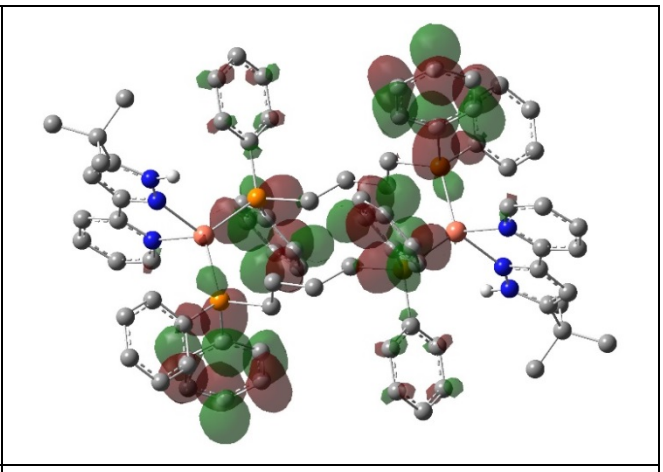
LUMO+13	LUMO+12
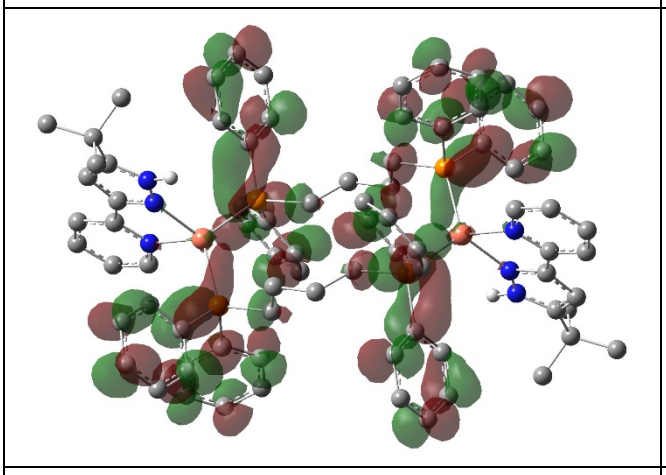	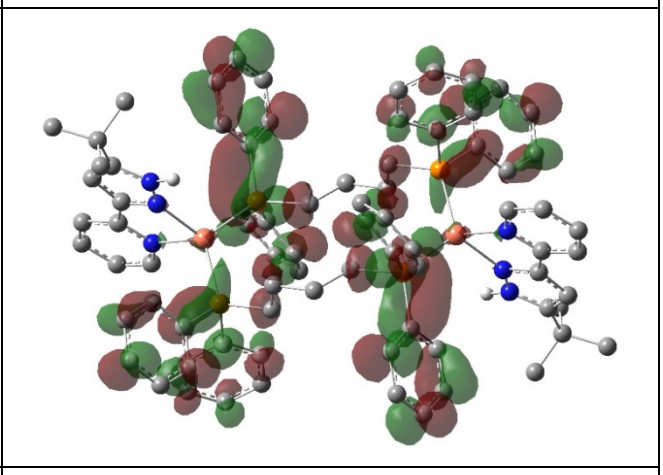
LUMO+5	LUMO+4
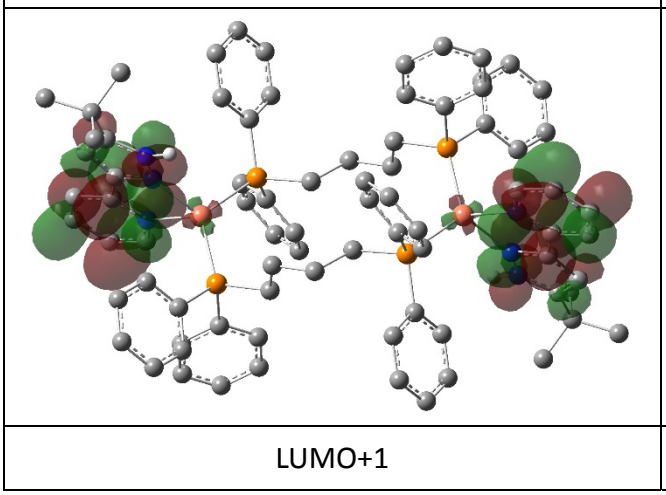	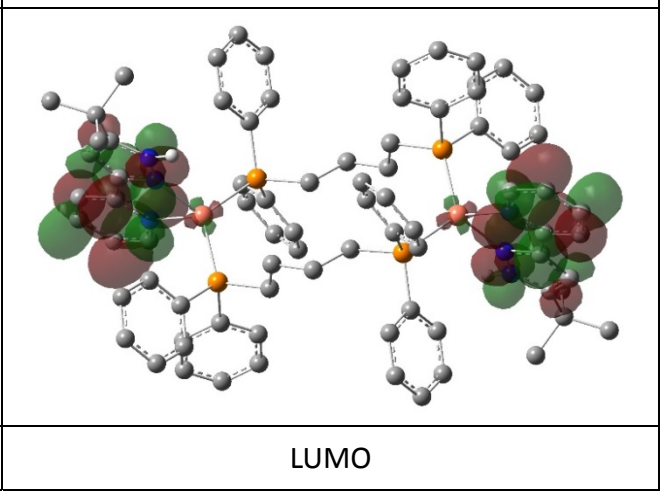
LUMO+1	LUMO

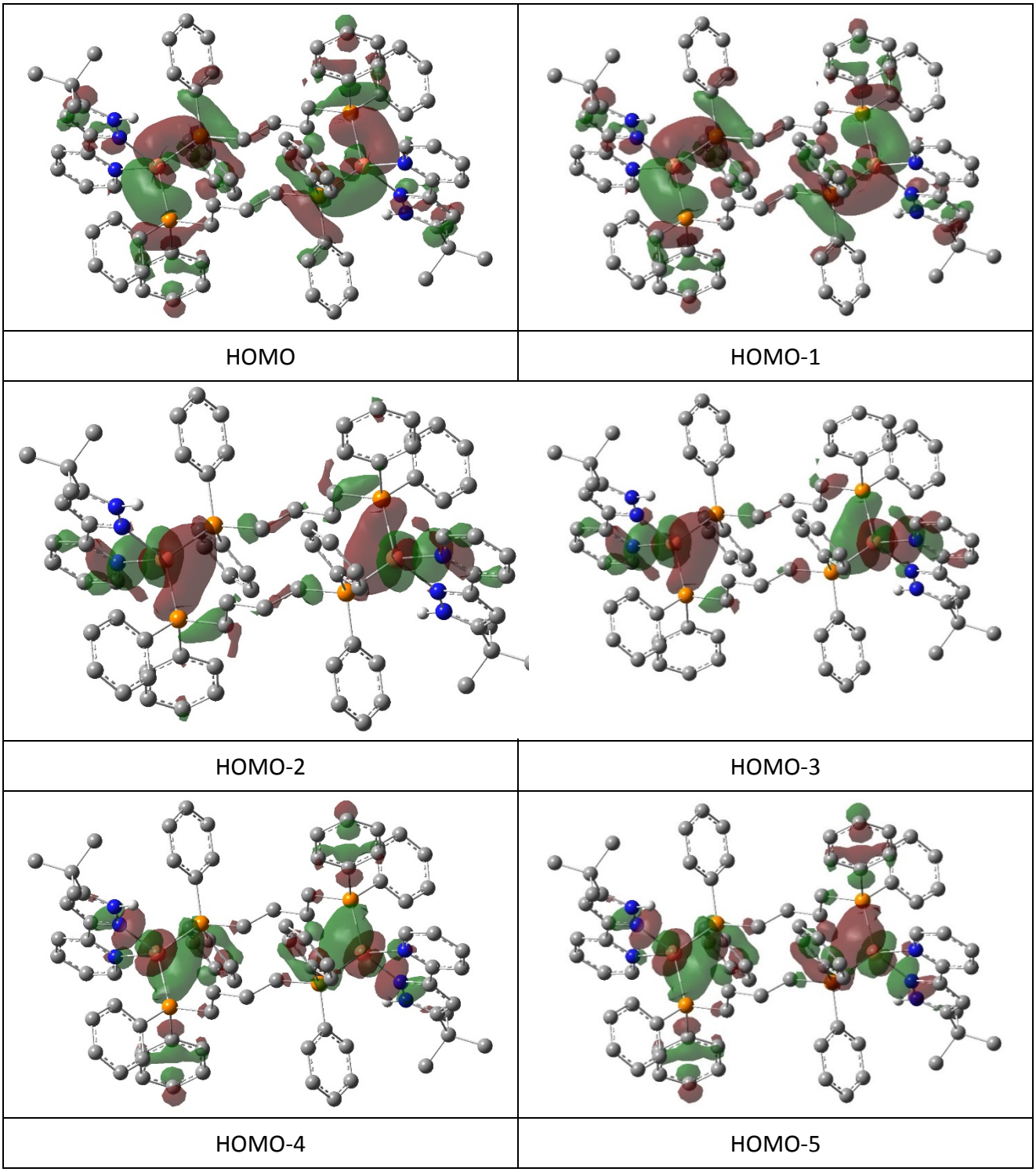

Figure S13 Plots of the frontier molecular orbitals involved in the absorption transitions of **2** in CH_2Cl_2 solution by TDDFT method at the B3LYP level (isovalue = 0.02). For clarity, the hydrogen atoms except for the ones bonded to N atoms are omitted. The red and green parts represent different phases, respectively.

Table S3 Partial molecular orbital compositions (%) by SCPA approach (C-squared population analysis proposed by Ros and Schuit) and the absorption transitions for **3** in CH_2Cl_2 solution calculated by TDDFT method at the B3LYP level.

orbital	energy (eV)	MO contribution (%)		
		Cu (s/p/d)	dppb	pyfpzH
LUMO+9	-1.03	5.55 (45/41/15)	80.12	14.33
LUMO+8	-1.04	4.97 (41/44/15)	88.97	6.05
LUMO+1	-2.17	2.08 (1/12/87)	3.83	94.08
LUMO	-2.18	2.09 (1/11/88)	3.73	94.19
HOMO	-6.27	41.10 (0/7/92)	54.70	4.20
HOMO-1	-6.28	41.65 (0/7/93)	54.13	4.22
HOMO-2	-6.56	59.33 (4/4/92)	26.29	14.38
HOMO-3	-6.59	61.01 (3/4/93)	23.75	15.25
HOMO-18	-7.50	19.16 (0/1/99)	69.70	11.14
HOMO-19	-7.50	21.55 (1/1/99)	67.23	11.22

state	E/nm (eV)	O.S.	transition	assignment	measured value (nm)
S_1	364 (3.40)	0.1300	HOMO-1→LUMO+1 (38%) HOMO→LUMO (37%) HOMO-3→LUMO (10%) HOMO-2→LUMO+1 (10%)	^{1}LLCT/^{1}MLCT/^{1}IL	340
S_3	359 (3.45)	0.0672	HOMO-2→LUMO+1 (30%) HOMO-3→LUMO (30%) HOMO→LUMO (13%) HOMO-1→LUMO+1 (10%)	^{1}MLCT/^{1}LLCT/^{1}IL	
S_{28}	272 (4.56)	0.2562	HOMO→LUMO+8 (37%) HOMO-1→LUMO+9 (33%)	^{1}IL/^{1}MLCT	270
S_{50}	260 (4.77)	0.3671	HOMO-19→LUMO+1 (16%) HOMO-18→LUMO (14%)	^{1}LLCT/^{1}MLCT/^{1}IL	

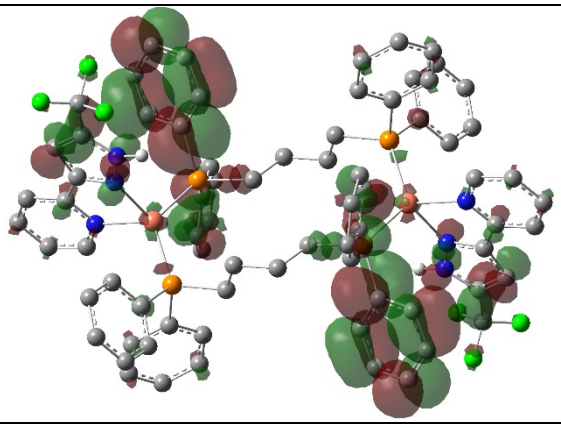	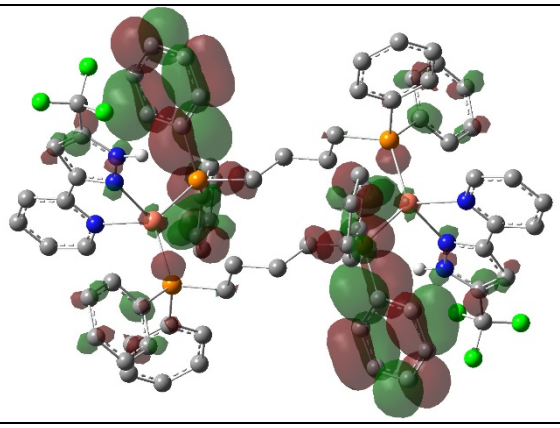
LUMO+9	LUMO+8
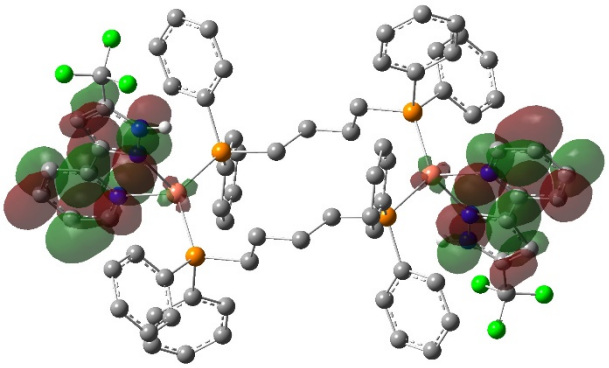	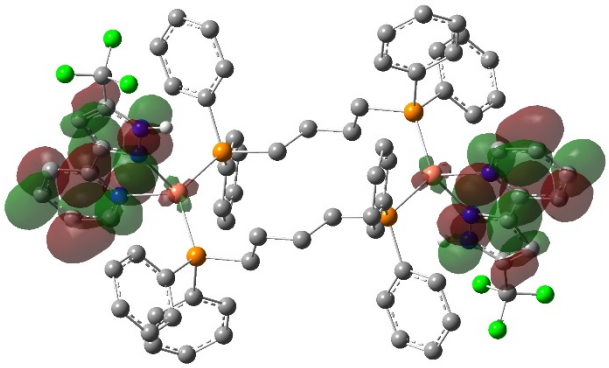
LUMO+1	LUMO
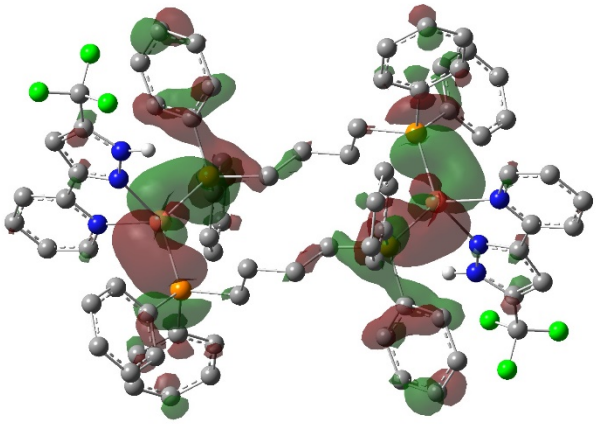	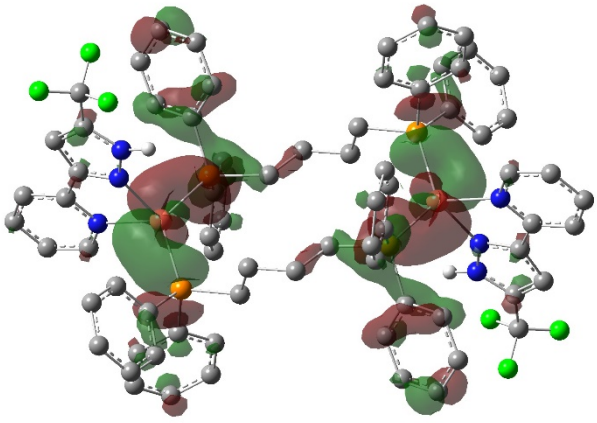
HOMO	HOMO-1

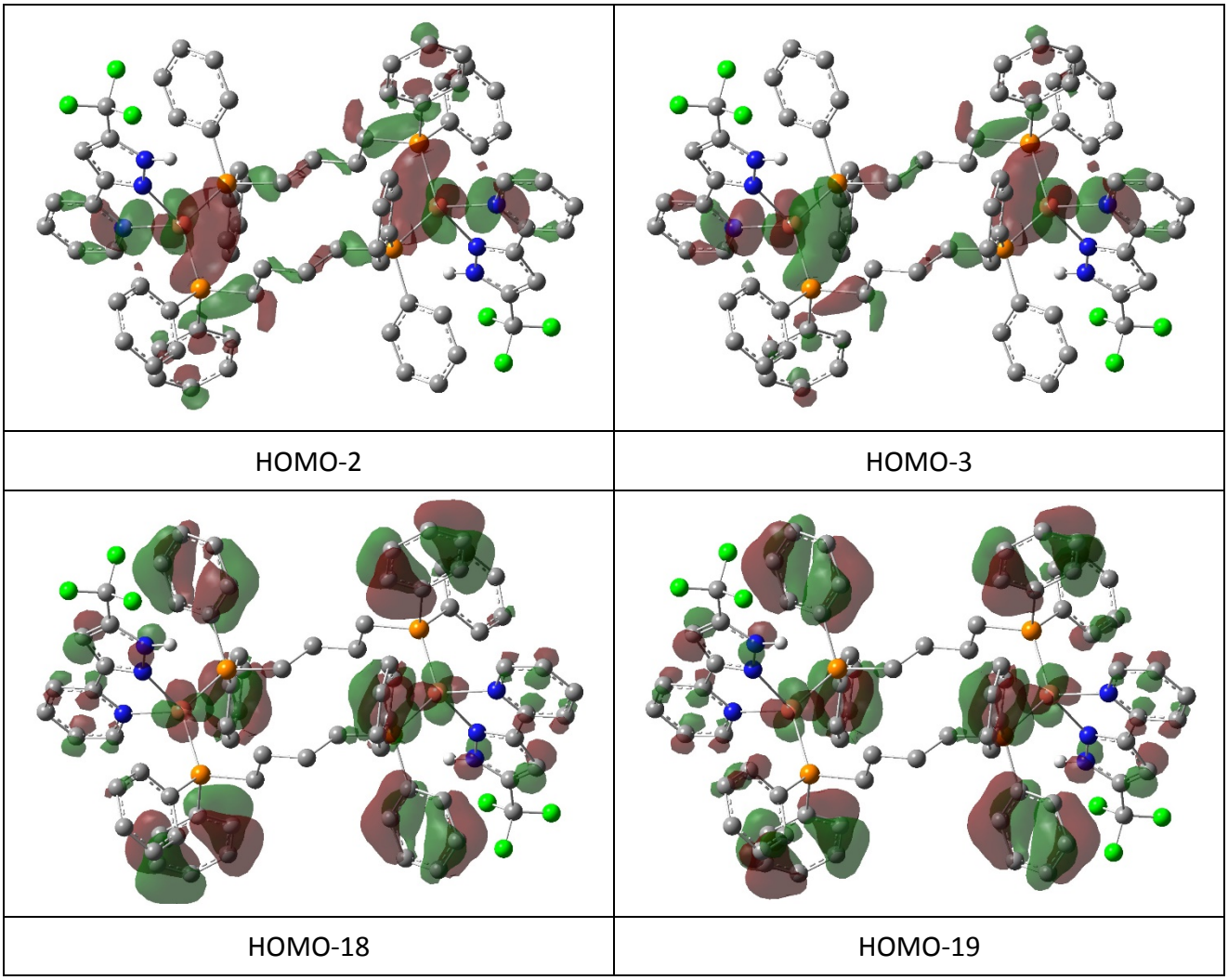

Figure S14 Plots of the frontier molecular orbitals involved in the absorption transitions of **3** in CH_2Cl_2 solution by TDDFT method at the B3LYP level (isovalue = 0.02). For clarity, the hydrogen atoms except for the ones bonded to N atoms are omitted. The red and green parts represent different phases, respectively.

Table S4 Partial molecular orbital compositions (%) by SCPA approach (C-squared population analysis proposed by Ros and Schuit) and the absorption transitions for the deprotonated derivative [{Cu(pyfpz)}$_2$(μ-dppb)$_2$] (**3-H**) of **3** in CH_2Cl_2 solution calculated by TDDFT method at the B3LYP level.

orbital	energy (eV)	MO contribution (%)		
		Cu (s/p/d)	dppb	pyfpz
LUMO+15	-0.42	2.56 (47/19/34)	95.21	2.24
LUMO+14	-0.43	5.69 (78/8/15)	91.64	2.68
LUMO+9	-0.57	3.52 (36/49/15)	90.96	5.52
LUMO+8	-0.59	4.33 (37/51/12)	92.31	3.36
LUMO+1	-1.13	2.34 (0/20/80)	5.17	92.48
LUMO	-1.13	2.28 (0/17/83)	4.72	93.00
HOMO	-5.48	43.12 (0/4/95)	44.43	12.45
HOMO-1	-5.49	43.48 (0/4/95)	44.12	12.40
HOMO-2	-5.62	55.07 (0/4/96)	7.24	37.69
HOMO-3	-5.62	54.23 (0/4/96)	7.23	38.54

state	E/nm (eV)	O.S.	transition	assignment
S_1	352 (3.52)	0.0030	HOMO-2→LUMO+1 (43%) HOMO-3→LUMO (42%)	^{1}MLCT/^{1}IL
S_3	339 (3.66)	0.1822	HOMO→LUMO (45%) HOMO-1→LUMO+1 (45%)	^{1}MLCT/^{1}LLCT/^{1}IL
S_{22}	293 (4.23)	0.2137	HOMO→LUMO+8 (46%) HOMO-1→LUMO+9 (42%)	^{1}IL/^{1}MLCT
S_{48}	278 (4.45)	0.1188	HOMO→LUMO+14 (31%) HOMO-1→LUMO+15 (30%)	^{1}IL/^{1}MLCT/^{1}LLCT

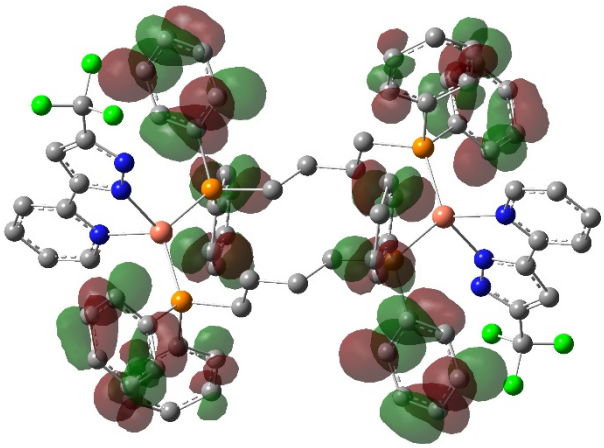	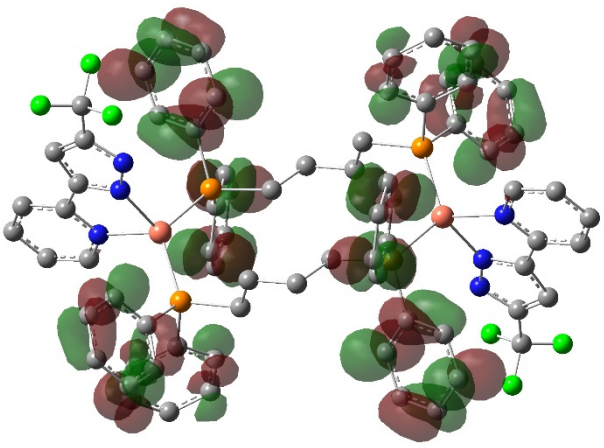
LUMO+15	LUMO+14
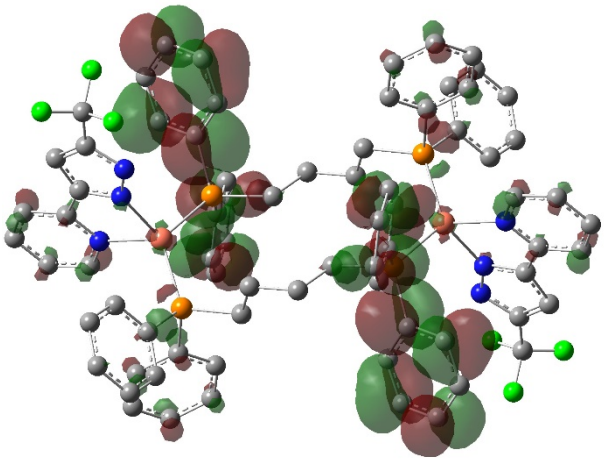	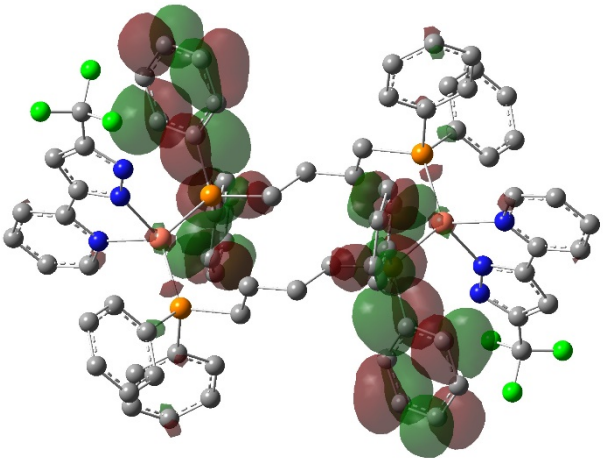
LUMO+9	LUMO+8
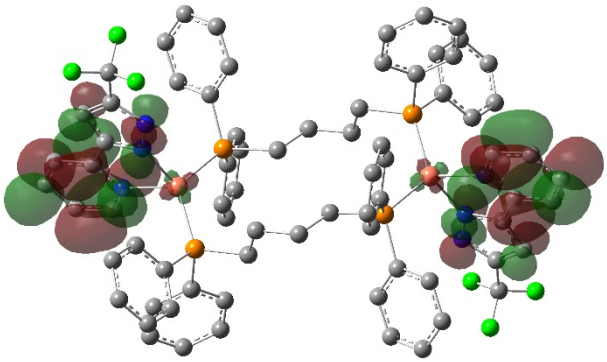	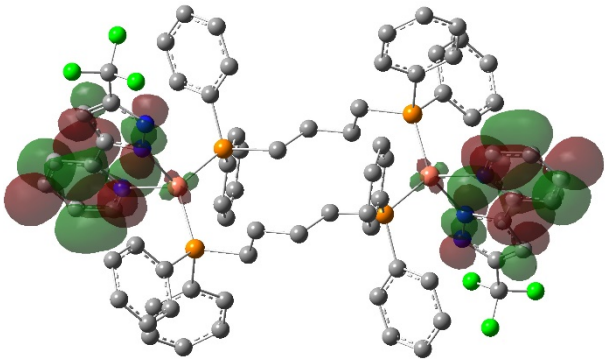
LUMO+1	LUMO

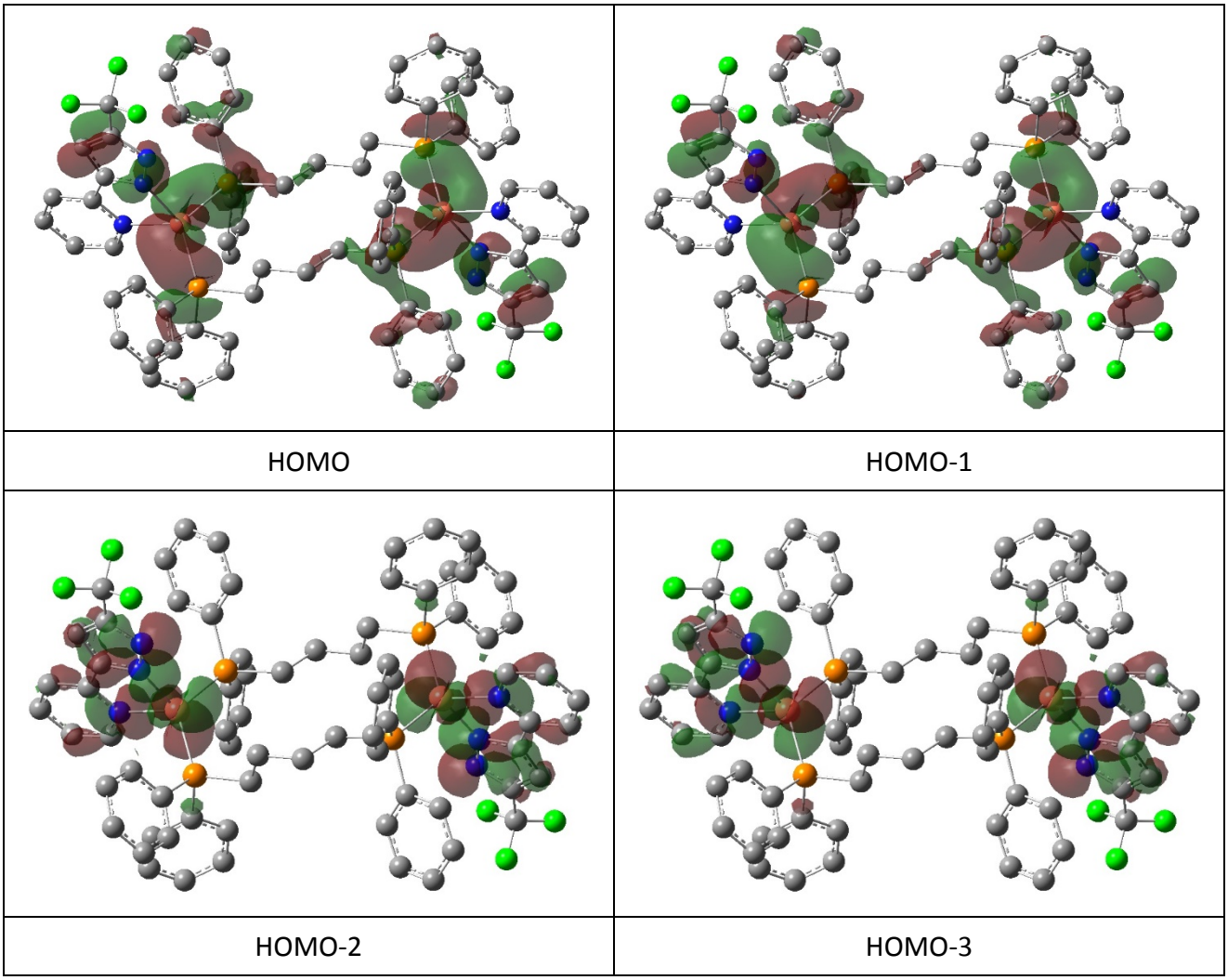

Figure S15 Plots of the frontier molecular orbitals involved in the absorption transitions of the deprotonated derivative [{Cu(pyfpz)}$_2$(μ-dppb)$_2$] (**3-H**) of **3** in CH_2Cl_2 solution by TDDFT method at the B3LYP level (isovalue = 0.02). For clarity, the hydrogen atoms are omitted. The red and green parts represent different phases, respectively.

Table S5 Partial molecular orbital compositions (%) by SCPA approach (C-squared population analysis proposed by Ros and Schuit) in the lowest triplet state for **1**–**3** and the deprotonated derivative [{Cu(pyfpz)}$_2$(μ-dppb)$_2$] (**3-H**) of **3**, respectively, in CH_2Cl_2 solution calculated by TDDFT method at the B3LYP level.

orbital	energy (eV)	MO contribution (%)		
1		Cu (s/p/d)	dppb	pypzH
LUMO+1	-2.88	3.19 (0/10/90)	4.89	91.92
LUMO	-2.88	3.20 (0/9/91)	5.08	91.73
HOMO	-5.34	71.58 (0/3/97)	7.68	20.74
HOMO-1	-5.34	71.20 (0/3/97)	8.14	20.66
2		Cu (s/p/d)	dppb	pybpzH
LUMO+1	-2.92	3.25 (0/9/91)	4.98	91.76
LUMO	-2.92	3.26 (0/9/91)	4.97	91.77
HOMO	-5.40	64.29 (0/3/97)	18.21	17.50
HOMO-1	-5.40	63.07 (0/3/97)	20.22	16.71
3		Cu (s/p/d)	dppb	pyfpzH
LUMO+1	-3.05	3.38 (0/7/93)	4.46	92.15
LUMO	-3.06	3.41 (0/7/93)	4.39	92.19
HOMO	-5.49	57.54 (0/4/96)	31.21	11.25
HOMO-1	-5.49	50.71 (0/5/95)	42.49	6.80
HOMO-2	-5.51	63.82 (0/3/97)	20.50	15.67
3-H		Cu (s/p/d)	dppb	pyfpz
LUMO+1	-1.93	2.87 (0/13/87)	4.75	92.37
LUMO	-1.93	2.85 (0/12/88)	4.44	92.71
HOMO	-4.52	59.00 (0/4/95)	8.66	32.34
HOMO-1	-4.52	58.76 (0/4/95)	8.97	32.27

Table S6 The emission transitions for **1**–**3** and the deprotonated derivative [{Cu(pyfpz)}$_2$(μ-dppb)$_2$] (**3-H**) of **3**, respectively, in CH_2Cl_2 solution calculated by TDDFT method at the B3LYP level.

state	E/nm (eV)	O.S.	transition	assignment	measured value (nm)
			1		
T_1	521 (2.38)	0	HOMO→LUMO (51%) HOMO-1→LUMO+1 (49%)	^{3}MLCT/^{3}IL	549
			2		
T_1	517 (2.40)	0	HOMO→LUMO (53%) HOMO-1→LUMO+1 (46%)	^{3}MLCT/^{3}IL/^{3}LLCT	536
			3		
T_1	528 (2.35)	0	HOMO-1→LUMO (50%) HOMO→LUMO+1 (37%) HOMO-2→LUMO+1 (11%)	^{3}MLCT/^{3}LLCT/^{3}IL	533
			3-H		
T_1	493 (2.51)	0	HOMO→LUMO (51%) HOMO-1→LUMO+1 (49%)	^{3}MLCT/^{3}IL	

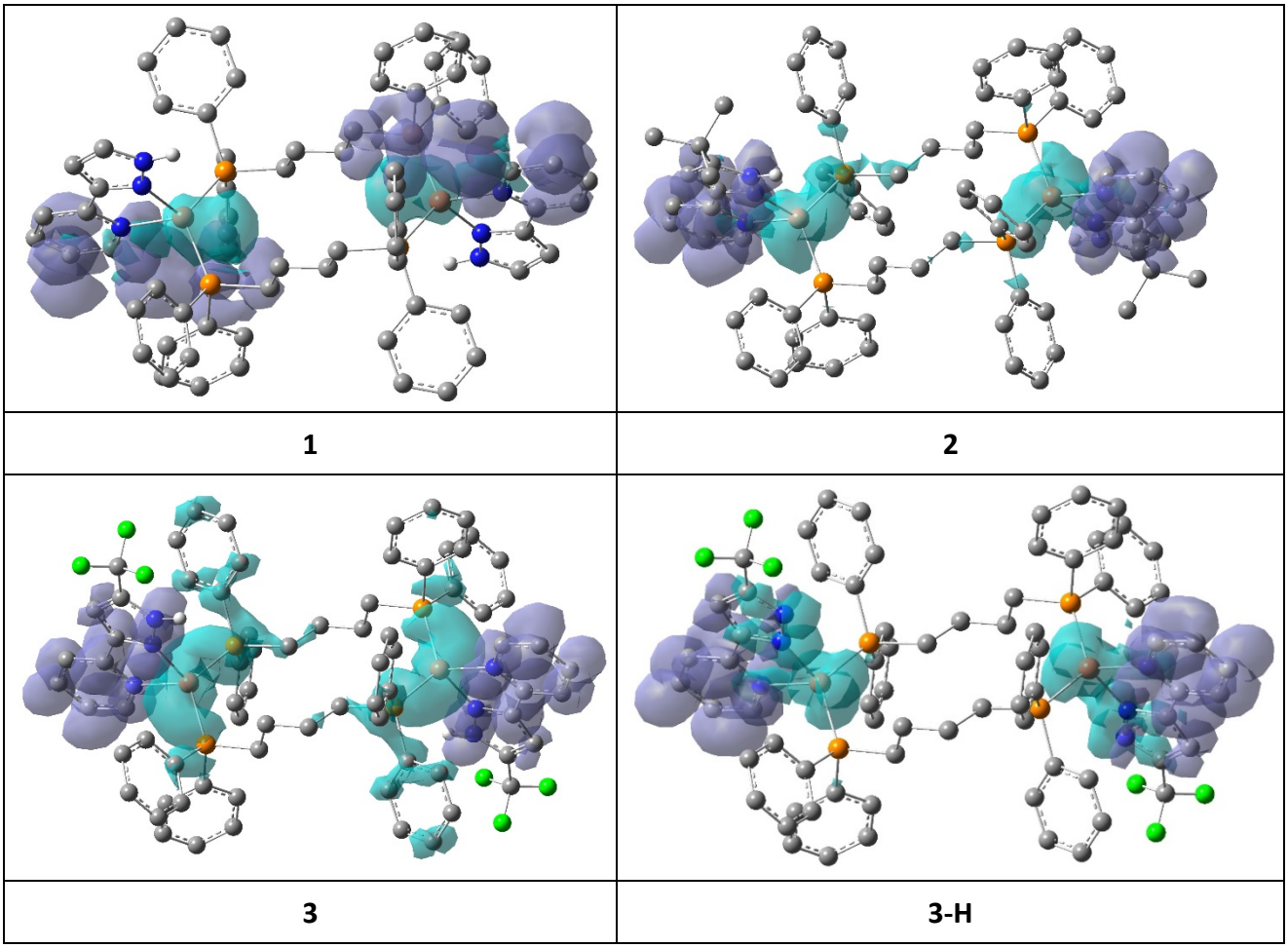

Figure S16 Plots of charge density difference map (isovalue = 0.0004) between lowest-energy triplet states T_1 and the ground states S_0 for **1**–**3** and the deprotonated derivative [{Cu(pyfpz)}$_2$(μ-dppb)$_2$] (**3-H**) of **3**, respectively, in CH_2Cl_2 solution calculated by TDDFT method at the B3LYP level. The purple and green parts display the electron accumulation and depletion region, respectively. For clarity, the hydrogen atoms except for the ones bonded to N atoms are omitted.

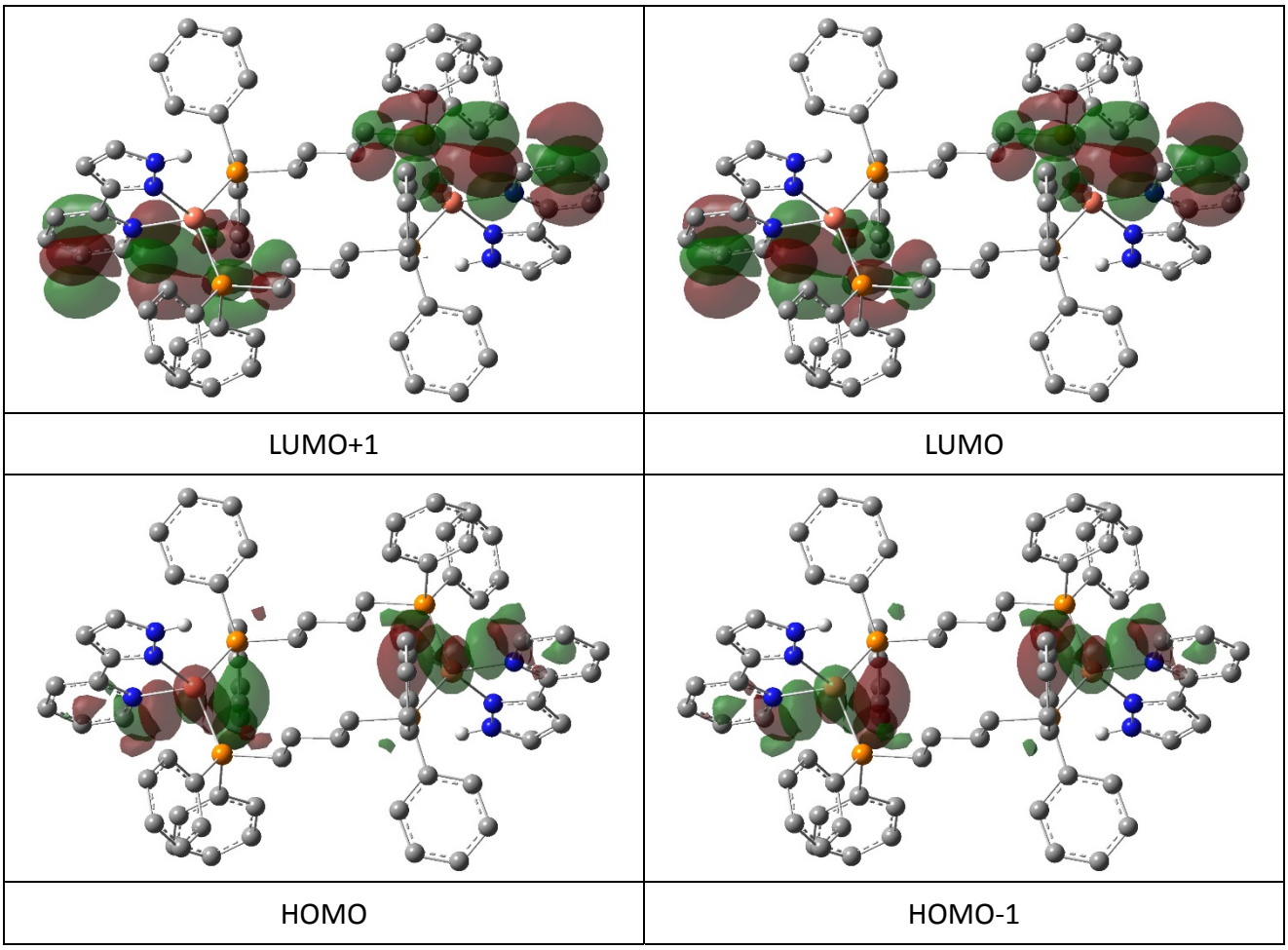

Figure S17 Plots of the frontier molecular orbitals involved in the emission transitions of **1** in CH_2Cl_2 solution by TDDFT method at the B3LYP level (isovalue = 0.02). For clarity, the hydrogen atoms except for the ones bonded to N atoms are omitted. The red and green parts represent different phases, respectively.

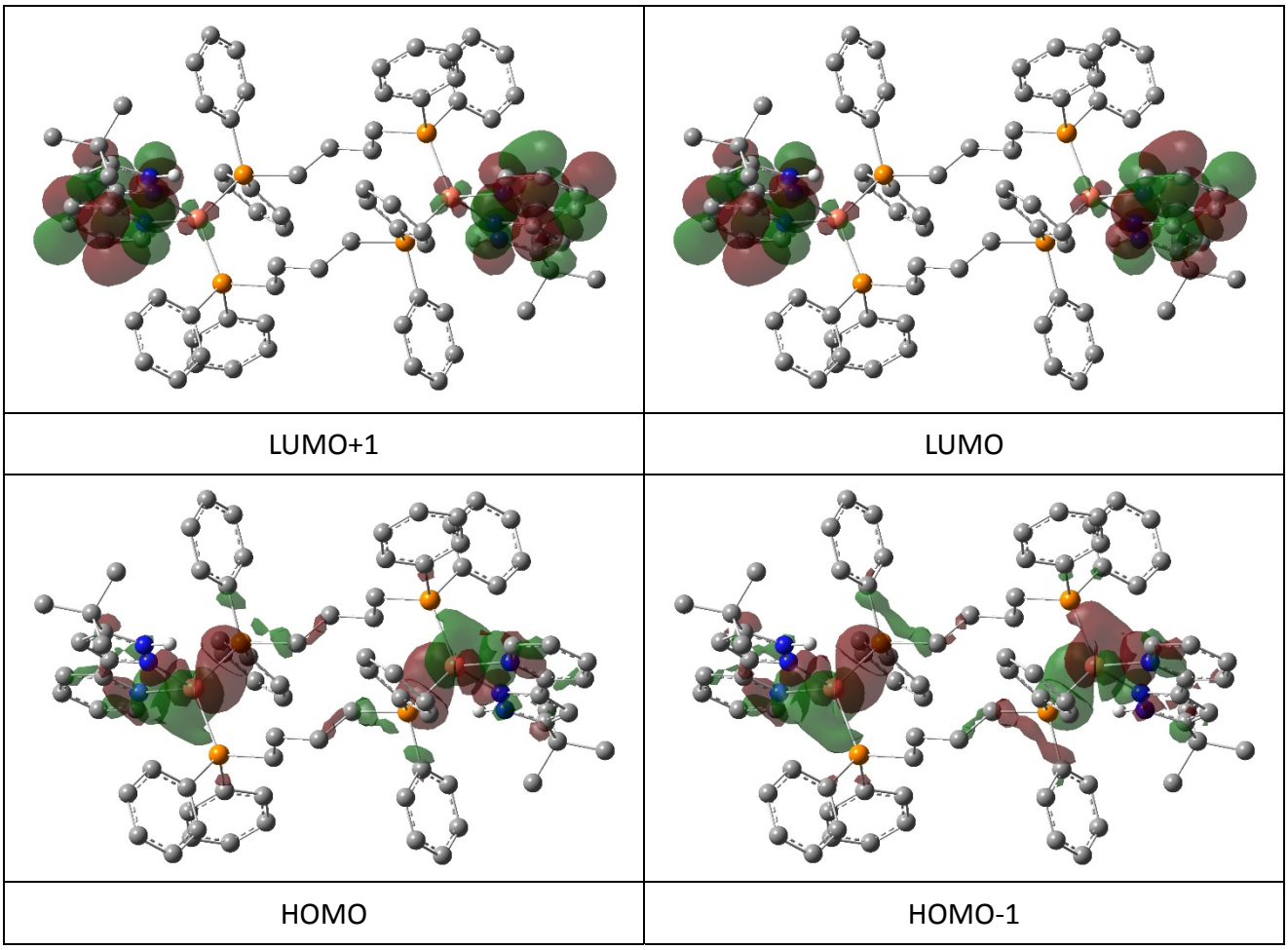

Figure S18 Plots of the frontier molecular orbitals involved in the emission transitions of **2** in CH_2Cl_2 solution by TDDFT method at the B3LYP level (isovalue = 0.02). For clarity, the hydrogen atoms except for the ones bonded to N atoms are omitted. The red and green parts represent different phases, respectively.

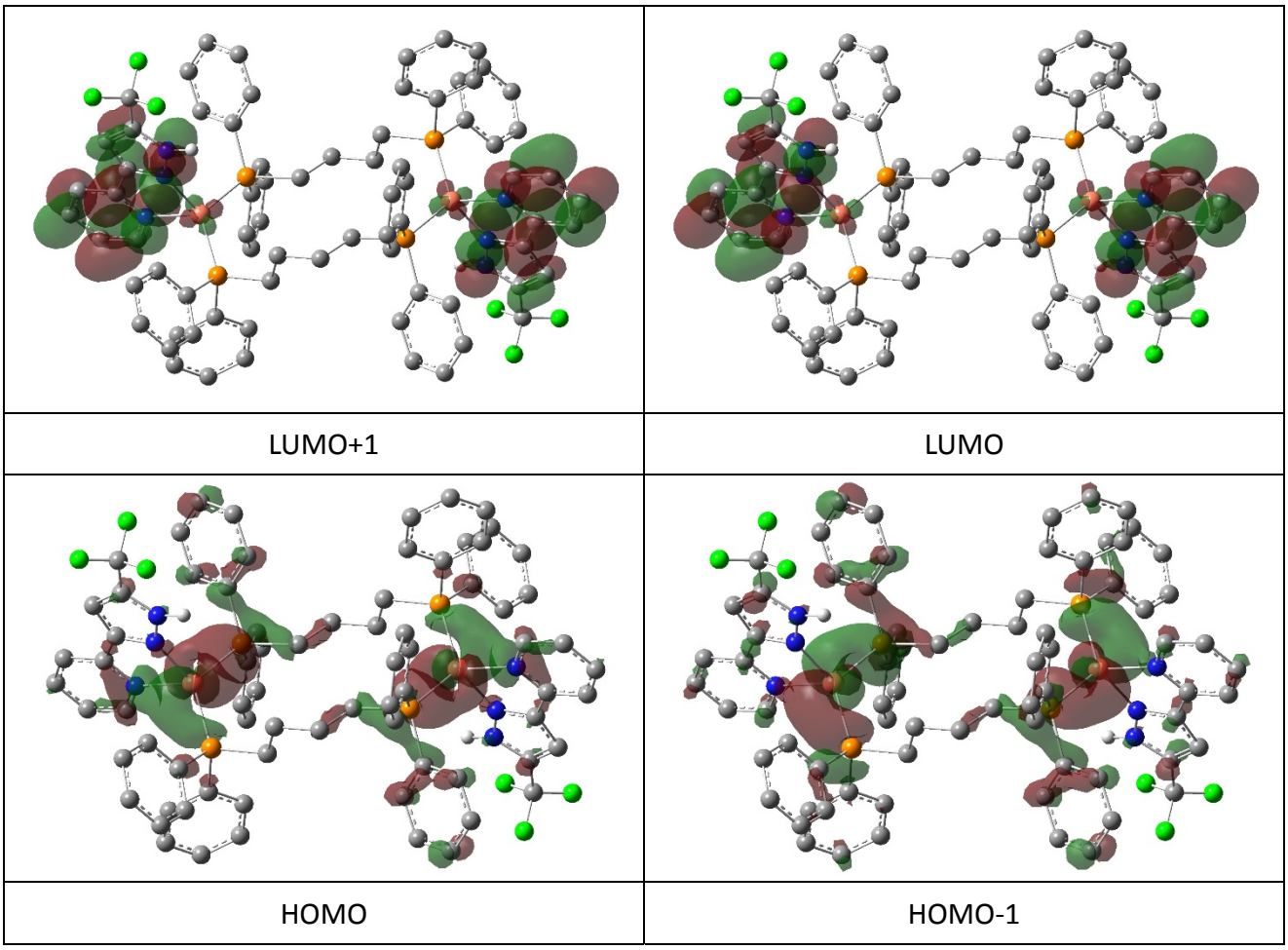

Figure S19 Plots of the frontier molecular orbitals involved in the emission transitions of **3** in CH_2Cl_2 solution by TDDFT method at the B3LYP level (isovalue = 0.02). For clarity, the hydrogen atoms except for the ones bonded to N atoms are omitted. The red and green parts represent different phases, respectively.

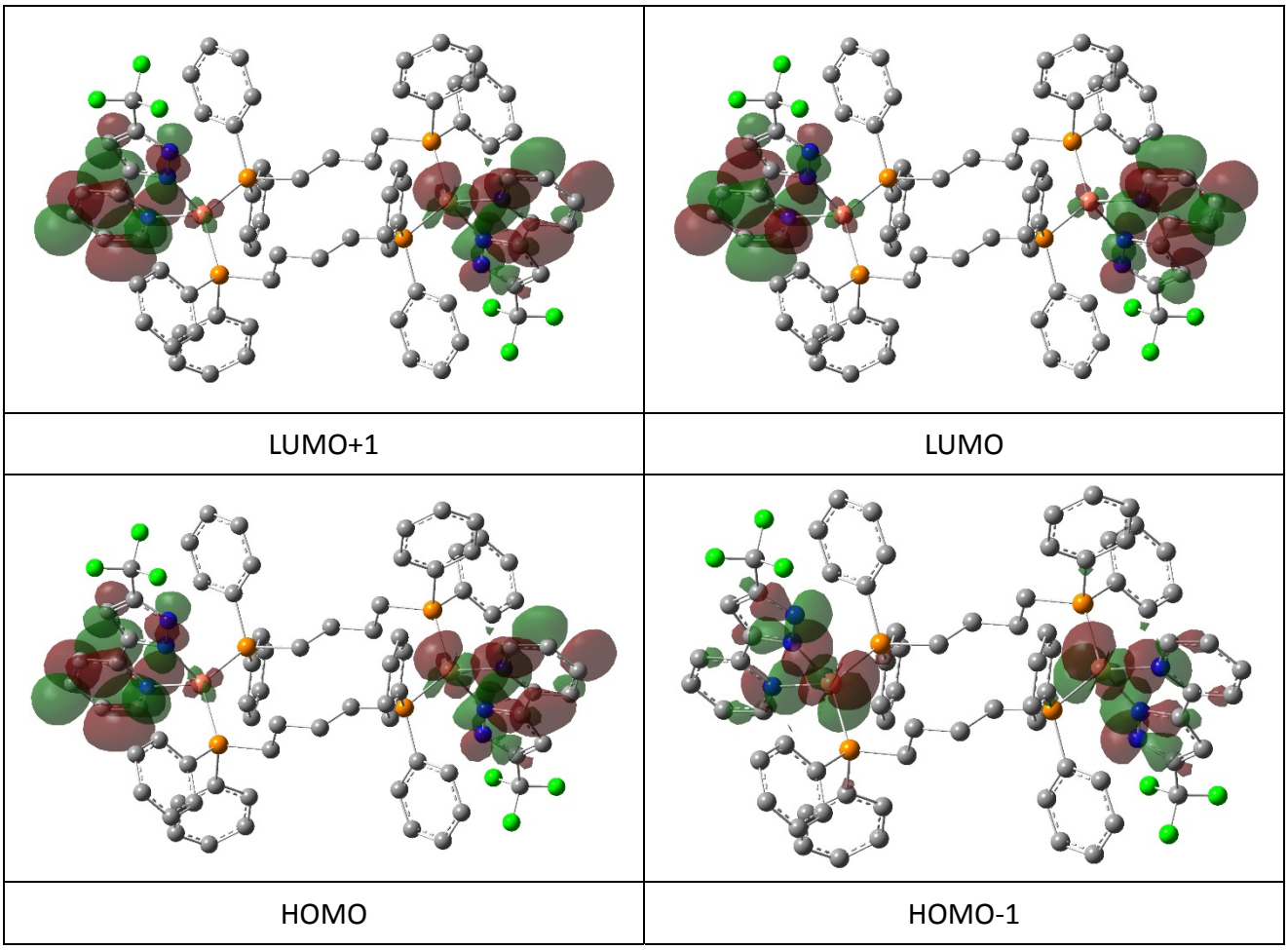

Figure S20 Plots of the frontier molecular orbitals involved in the emission transitions of the deprotonated derivative [{Cu(pyfpz)}$_2$(μ-dppb)$_2$] (**3-H**) of **3** in CH_2Cl_2 solution by TDDFT method at the B3LYP level (isovalue = 0.02). For clarity, the hydrogen atoms are omitted. The red and green parts represent different phases, respectively.

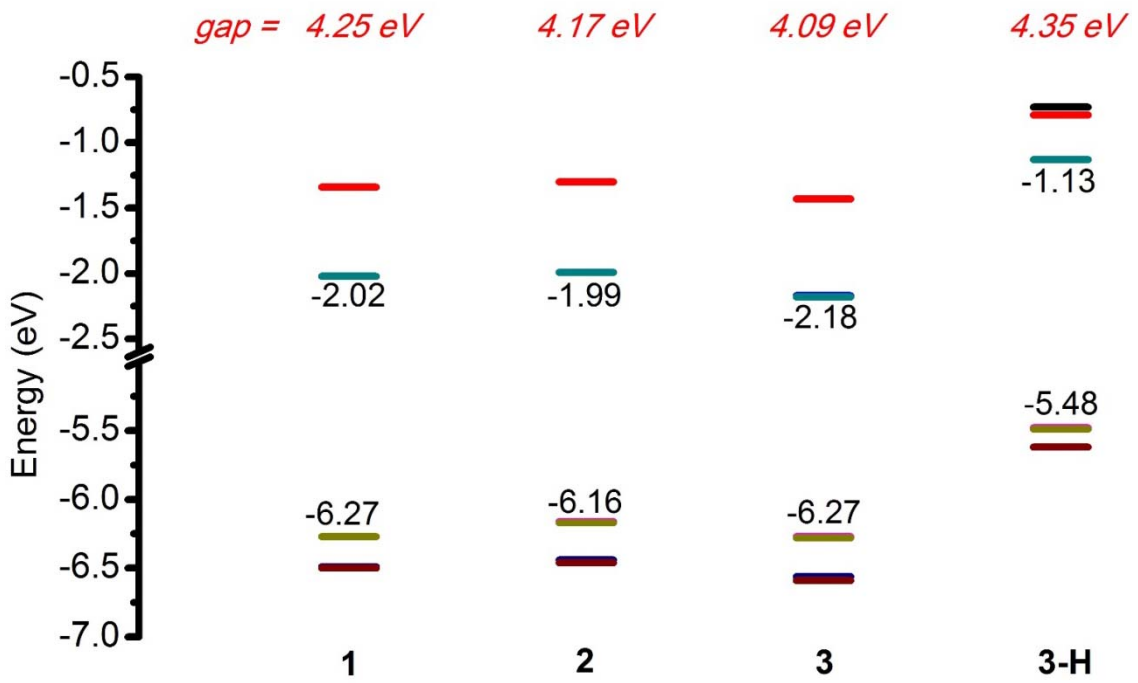

Figure S21 Plots of energy level of frontier orbitals in the ground states for **1**–**3** and the deprotonated derivative [{Cu(pyfpz)}$_2$(μ-dppb)$_2$] (**3-H**) of **3**, respectively, in CH_2Cl_2 solution by TDDFT method at the B3LYP level.

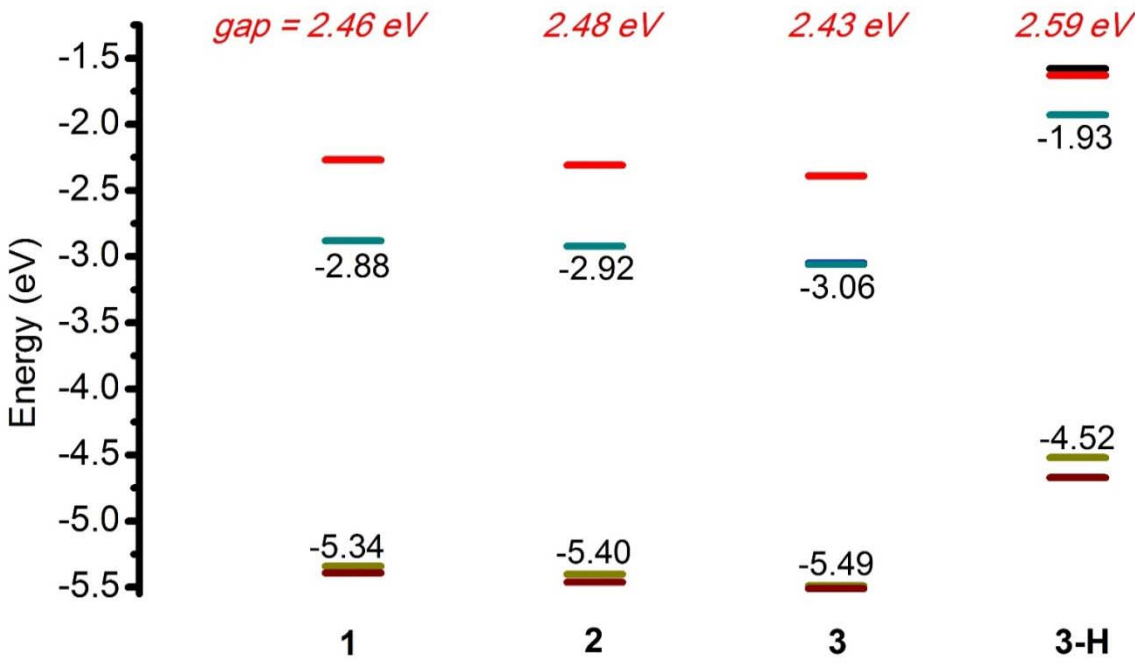

Figure S22 Plots of energy level of frontier orbitals in the lowest triplet states for **1**–**3** and the deprotonated derivative [{Cu(pyfpz)}$_2$(μ-dppb)$_2$] (**3-H**) of **3**, respectively, in CH_2Cl_2 solution by TDDFT method at the B3LYP level.

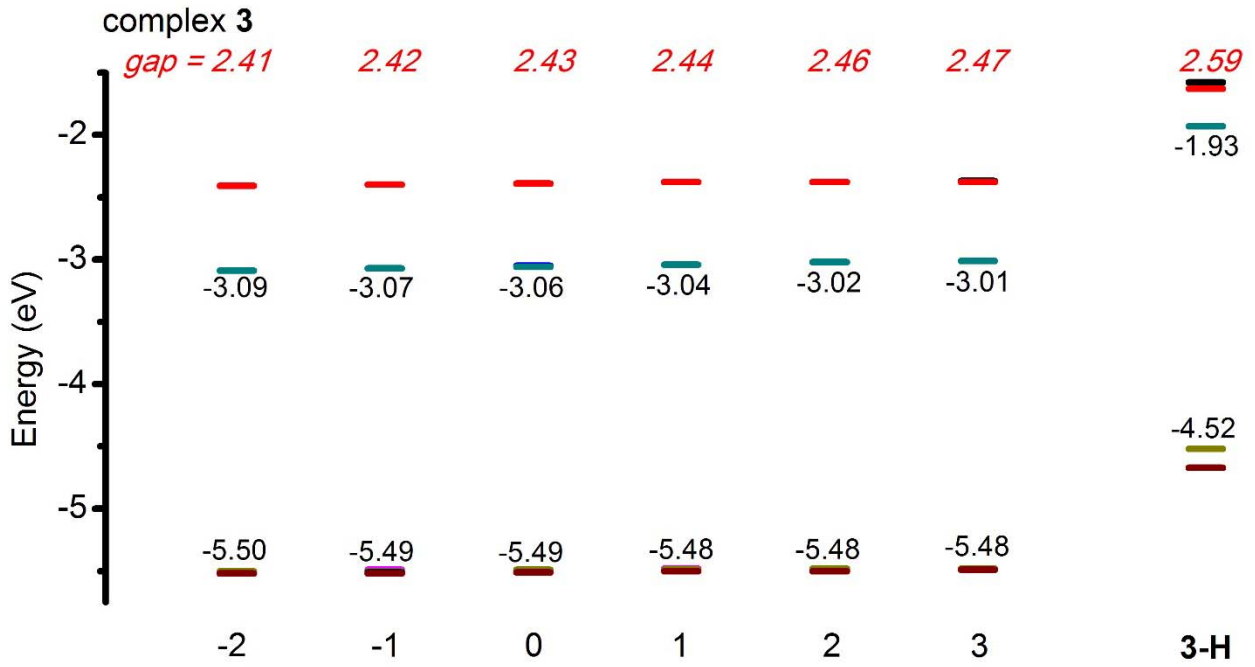

Figure S23 Plots of energy level of frontier orbitals in the lowest triplet states for **3** by changing the N–H bond length (-2, -1, 0, 1, 2, 3 denote the N–H bond length of 0.817, 0.917, 1.017, 1.117, 1.217, and 1.317 Å, respectively), in CH_2Cl_2 solution by TDDFT method at the B3LYP level.